Comparison of pleural lesions using vibrational spectroscopy

Sadiku Zehri, Fatlinda

UNIVERSITY OF ZAGREB

SCHOOL OF MEDICINE

Fatlinda Sadiku Zehri

Comparison of pleural lesions using vibrational spectroscopy

Dissertation

Zagreb, 2020

UNIVERSITY OF ZAGREB

SCHOOL OF MEDICINE

Fatlinda Sadiku Zehri

Comparison of pleural lesions using vibrational spectroscopy

DISSERTATION

Zagreb, 2020

This PhD thesis was carried out at the Institutes of Pathology and Physics and Biophysics of the School of Medicine - University of Zagreb

Mentors: Prof. Sven Seiwerth MD. PhD.
Ass. Prof. Ozren Gamulin PhD.

Acknowledgements

I wish to express my deep gratitude to my mentors, Prof. Dr. Sven Seiwerth and Ass. Prof. Ozren Gamulin, as well as late Ass. Prof. Maja Balarin for their unconditional support and guidance.

I would like to thank the staff of the Departments of Pathology and Physics and Biophysics at the Medical School of the University of Zagreb, with special thanks to Mrs. Djurdja Poljan for her help.

I would also like to thank my family for the continuous support and encouragement to always aim high.

DEDICATION

To my grandmother and grandfather, who would be very happy and proud.

To my parents, for their unconditional love and support.

To my sons Fron and Mat, for existing.

CONTENT

1. INTRODUCTION ……...……1

1.1. Pleura……..7

1.1.1. Mesothelial reactive changes.....8

1.1.2. Tumours of pleura 9

1.1.2.1. Malignant mesothelioma.....9

1.1.2.1.1. Epidemiology 10

1.1.2.1.2. Etiology and pathogenesis 10

1.1.2.1.3. Clinical features 12

1.1.2.1.4. Macroscopy and localisation.....13

1.1.2.1.5. Histopathology 14

1.1.2.1.6. Spread and staging 16

1.1.2.1.7. Treatment 17

1.1.2.1.8. Prognosis 18

1.1.3. Metastatic tumours of pleura ……..……18

1.1.3.1. Lung tumours ……19

1.1.3.1.1. Lung adenocarcinoma …….……19

1.1.3.1.1.1. Etiology and epidemiology ……..…..…..…19

1.1.3.1.1.2. Clinical features ……...20

1.1.3.1.1.3. Macroscopy, localisation and histopathology …….20

1.1.3.1.1.4. Spread and staging …….……..21

1.2. Diagnostic methods ……..21

1.2.1. Immunohistochemistry ……22

1.2.2. Electron microscopy ……24

1.2.3. Vibrational spectroscopy ……..…24

2. HYPOTHESIS……26

3. AIMS OF THE STUDY ..……27

3.1. General aim……..27

3.2. Specific aims ……...27

4. MATERIALS AND METHODS ……..……..……28

4.1 Tissue samples ……28

4.2 FTIR spectroscopy ……..……29

4.3 Data analysis ……31

5. RESULTS ……..…….33

5.1 Histopathological evaluation ……...……33

5.2 FTIR spectra ……38

5.3 Student`s T-test ……41

5.4 Principal Component Analysis ……45

5.5 Unknown sample spectra identification and model validation ……...……50

5.6 Loadings ……..…52

6. DISCUSSION ……54

7. CONCLUSION ……..…….59

8. SAŽETAK (ABSTRACT IN CROATIAN) ..……..……60

9. ABSTRACT ……...……61

10. REFERENCES ……..62

11. CURRICULUM VITAE ……..…..76

SYMBOLS AND ABBREVIATIONS

WT-1 -	Wilms tumour 1
CK 5/6 -	Cytoceratin 5/6
CEA -	Carcinoembrionic antigen
TTF-1 -	Thyroid transcription factor 1
EMA -	Epithelial membrane antigen
CD15 -	Cluster of differentiation 15
HBME-1 -	Hector Battifora mesothelial-1
LeuM1 -	Mouse monoclonal CD15 antibody
CD147 -	Cluster of differentiation 147
GLUT-1 -	Glucose transporter 1
BAP-1 -	BRCA1 Associated Protein 1
FISH -	Fluorescence in situ hybridisation
MTAP -	Methylthioadenosine phosphorylase
CD47 -	Cluster of differentiation 47
FTIR -	Fourier transform infrared spectrometer
IR -	Infrared
mid-IR -	mid-Infrared
NILM -	Negative for Intraepithelial Lesion or Malignancy
LSIL -	Low-grade squamous intraepithelial lesion
HSIL -	High-grade squamous intraepithelial lesion
WHO -	World Health Organisation
TNF-α -	Tumour necrosis factor α
IL-β1 -	Interleukin β1
NF-κB -	Nuclear factor kappa-light-chain-enhancer of activated B cells
DNA -	Deoxyribonucleic acid
SV40 -	Simian virus
CT -	Computed tomography
MRI -	Magnetic resonance imaging
PET -	Positron emission tomography
PNET -	Primitive neuroectodermal tumour
MFH -	Malignant fibrous histiocytoma
TNM -	Tumour, node and metastasis

UICC -	Union for International Cancer Control
LDH -	Lactate dehydrogenase
CD10 -	Cluster of differentiation 10
PCA -	Principal component analysis
PC1 -	Principal component 1
PC2 -	Principal component 2
STT -	Student`s T test
IHC -	Immunohistochemistry
HE -	Haematoxylin & Eosin
CLL -	Chronic lymphocytic leukaemia

1. INTRODUCTION

Currently, despite its subjectivity, histopathological evaluation remains the "golden standard" in diagnostics (1,2). Microscopic criteria that differentiate benign from malignant cells in general are based on morphology, size of the cells, size of the nucleus (larger in the tumour cells) and invasion of surrounding normal tissue (1). Even though the criteria exists the similarity between tumours, the diversity of histological patterns in respective tumours and the poor differentiation of tumour cells lead to diagnostic difficulties and/or misdiagnosis. Immunohistochemistry is a method that elucidates the origin of the tumour cell. However, in some occasions, it fails to differentiate between benign and malignant nature of the cells.

Malignant mesothelioma is a rare tumour with a very poor prognosis and with a tendency of increased incidence (3,4). The morphological challenges to objectively diagnose this type of tumour is worrisome since histological patterns of malignant mesothelioma can imitate the appearance of many epithelial and non-epithelial malignancies (5). Furthermore, some reactive changes of mesothelial cells can also mimic malignant mesothelioma (2,5–7). Reactive mesothelial changes that can mimic malignancy can be seen in infection, infarction, systemic diseases, inflammatory changes, radiotherapy, chemotherapy, liver diseases, and also in secondary changes associated with primary or metastatic tumours (8).

Special challenges are found when differentiating reactive mesothelial hyperplasia from epithelioid malignant mesothelioma and reactive pleural fibrosis from sarcomatoid mesothelioma, because mesothelial hyperplasia, cellular atypia and entrapment of these mesothelial cells under the pleural surface found on these changes can be difficult to properly appreciate (9).

To date, immunohistochemistry is very important in differential diagnosis between malignant pleural mesothelioma, primary lung adenocarcinoma and metastatic tumors (6). Standard immunohistochemical panel includes antibodies specific to mesothelium such as: Calretinin, Thrombomodulin, WT-1, D2-40, CK 5/6, mesothelin. Negative markers for mesothelial cells are CEA, TTF-1, MOC-31, BerEp4 (10–15). A panel, including at least two positive and two negative markers, helps in identifying lesions of mesothelial origin (10).

In the endeavours to find a marker that will differentiate mesothelioma from reactive mesothelial proliferation, keratin, p53, EMA and desmin have been used, however overlapping results have hampered these attempts (16). The same paper presented the panel

for diagnosis of malignant mesothelioma consisting of Calretinin, WT-1, Cytokeratin 5/6, TTF-1, CEA and B72.3 (16).

A comparative study by Ordonez showed that the panel should consist of two positive and two negative markers. The preferred combination was: Calretinin and Cytokeratin 5/6 (or WT1) being positive, and CEA with MOC-31 being negative (17).

Struggling to find a proper panel for differentiating mesothelioma from adenocarcinoma, Comin *et al.*, concluded that positive markers Calretinin and Thrombomodulin, and negative markers CD15 and CEA, could be the initial first hand antibodies in discrimination between mesothelioma and lung adenocarcinoma (15).

In the met analysis of 88 studies by King *et al.*, which used immunohistochemistry for differentiating between malignant mesothelioma from metastatic lung adenocarcinoma in pleura, 15 markers were analysed and the results have shown that MOC-31 and BG8 were the most sensitive, while CEA and TTF-1 the most specific for diagnosis of adenocarcinoma. For the diagnosis of malignant mesothelioma the most sensitive markers proved to be CK5/6 and HBME-1, and the most specific were WT1 and CK5/6 (18).

In a retrospective study by Sandeck *et al.*, the most reliable imunohistochemical markers in histopathological re-evaluation of malignant mesothelioma cases were shown to be Calretinin, EMA, CEA and BerEp4. But in 6 of 49 cases it was impossible to give a ”clear-cut diagnosis” (19).

Abutaily *et al.* re-evaluated 76 cases of lung adenocarcinoma and mesothelioma. Most sensitive imunohistochemical markers for adenocarcinoma were E-cadherin with a sensitivity of 100%, and most specific was shown to be TTF-1 with a specificity of 100%. When TTF-1 was negative and E-cadherine positive, secondary panel for distinction of adenocarcinoma from mesothelioma consisted of BerEp4, LeuM1, EMA, Calretinin, Cytokeratin 5/6, Thrombomodulin and N-cadherin (20).

Differentiating malignant from non-malignant mesothelial cells remains the main challenge in the diagnostics of pleural lesions. Immunohistochemical markers, CD147 and GLUT-1 have been used to discriminate between reactive and malignant mesothelial cells with a sensitivity of 88.8% and specificity of 90.9% (12).

Recent studies have analyzed possible markers for differentiating malignant from non-malignant mesothelial cells, such as loss of BAP-1 expression by immunohistochemistry and p16 deletion by FISH (*fluorescent in situ hybridization*). The data have shown high specificity (100%) and good sensitivity representing the currently applied standard diagnostic tool (21–26). Also, MTAP and BAP-1 immunohistochemistry in combination were shown to

be highly specific (100%) and sensitive (90%) for the diagnosis of malignant mesothelioma (27,28). There is a study in small tissue samples and pleural fluids that supports the idea of using the identification of BAP1 loss and p16 deletion by FISH, first for discriminating malignant from reactive mesothelial cells (29). There are two reported cases of mesothelioma in situ, based on the same molecular traits for BAP-1 and p16 found in cases with invasive mesothelioma, even though there were no histological criteria for malignancy (30).

In a study of Tochigi at al., was shown that deletion of p16 is very often finding in malignant mesothelioma, notably in sarcomatoid type, but because of the overlapping results it may not be used alone for differential diagnosis between sarcomatoid tumours of the lung and pleura (31). Because of the overlapping immunohistochemical results, International Mesothelioma Panel and MESOPATH National Reference Center highlighted the need of correlation of histology with clinical and imaging findings, in discriminating pleural sarcomatoid mesothelioma from sarcomatoid carcinomas (32).

Another study in mesothelial proliferations, highlights that deletion of p16 was not found in none of their cases, while 7% of those non-malignant changes were positive for GLUT-1 (33). Deletion of p16 in cytology samples of mesothelium was evaluated, presented that it may be reliable in differentiating between reactive and malignant mesothelial changes (34).

CD47 is a molecule that inhibits the phagocytosis and has been found to be overexpressed in malignant mesothelioma cells. This marker, in combination with BAP-1 loss has been shown to be sensitive (78%) and specific (100%) in differentiation between malignant mesothelioma and reactive mesothelial cells (35).

As there are no specific stains, the main challenge lies in differentiating between malignant and reactive mesothelial cells (18). Tumour invasion of the lung or surrounding fat and muscle currently remains the only criterion for malignancy (5,9,10,36).

Our approach evaluates vibrational spectroscopy as an analytical method and a possible diagnostic tool for pleural pathology. It has recently been shown that tumour cells can be distinguished from their normal counterparts by comparison of their Fourier Transform Infrared (FTIR) spectra (37–39). Vibrational spectroscopy is a well-established research analytical method based on the physical properties of matter (40). It analyses the interaction between the electromagnetic waves and the matter. Based on light absorption, this method helps in identifying the molecular nature of samples. Mid-infrared (mid-IR) spectral region with wavenumbers from 4000 to 400 cm^{-1} is the standard region of vibrational spectroscopy that holds the information for identification of organic molecules (41). The

principle of infrared spectroscopy is based on the fact that almost all molecules absorb infrared radiation (39). Furthermore, different tissues, cells or fluids have different biochemical content. Depending on the biochemical content, cells or tissues will absorb infrared radiation differently, and that will, therefore, result with different infrared spectra (42). FTIR spectroscopy can observe three parameters: intensity, band width and position of the vibrational band (40). The difference between those three parameters of vibrational bands in the infrared spectra generates the necessary information for differentiation between normal or abnormal cells and tissues (43). In other words, the different cells, or even different state of a cell, create different infrared spectra, identifying either their type or condition based on the different biochemistry of their compounds (44,45).

FTIR spectroscopy can support complex diagnoses of altered biochemistry at the cellular level (46).

FTIR spectroscopy offers many advantages in cancer diagnosis such as simplicity, shorter procedures, and is relatively a cost-effective process (47–49). This method was also used to distinguish other benign from malignant changes in organs such as colon, prostate, lung, breast, cervix, stomach, oral cavity, liver, skin, thyroid and oesophagus (43,50,51).

Red blood cells from patients with gastric carcinoma were compared with red blood cells of healthy subjects by FTIR spectroscopy, and the results have shown 84% accuracy, 95% sensitivity and 70% specificity, considering FTIR as a promising method in gastric cancer diagnostics (52).

FTIR spectroscopy has been used to analyse blood serum and plasma samples to detect biomarkers present in patients with non-small cell lung carcinoma and for differentiation between squamous cell carcinoma and adenocarcinoma. The subsequent results have been very promising for the use of FTIR in routine diagnostics (53).

In the pursuit to find a screening tool for lung cancer, FTIR spectra were used to compare sputum of cancer patients with healthy subjects. The data from those spectra divided the samples into two groups and have shown that FTIR has a high specificity and sensitivity in lung cancer diagnosis and is a promising method for screening (50).
In the study by Wang *et al.*, comparative analysis of pleural effusion cells in lung cancer and tuberculosis has been carried out. These results have shown real possibility for the use of FTIR spectroscopy as a rapid, cost effective and valuable diagnostic tool (47).

Results from a comparative study of normal and malignant liver cells, suggested that FTIR spectroscopy can be a diagnostic tool in liver cancer diagnosis (43).

FTIR spectroscopy was used for detection of sentinel lymph node metastases in breast carcinoma intraoperatively. In a study of 149 sentinel lymph nodes with metastatic cells, the results have shown that sensitivity, specificity and accuracy were above 90% (54). This evidence shows that the value of using this method during surgery is even higher in cases where the time for decision-making is very limited.

The accuracy in differentiating nodular goitre from thyroid carcinoma during intraoperative spectroscopy was 86.6% in one study (51).

According to a review article by Mitchell *et al.* about disease screening and diagnosis, FTIR spectroscopy is a very sensitive method in identifying malignant precursors and there should be a scope for using it in a routine clinical work in cancer and chronic diseases. The concept of using FTIR spectroscopy as a screening method for cancer is based in detecting the nucleic acids released from tumour cells in general circulation, in cancers that are in the asymptomatic stage (45). This supports the idea of standardization of diagnostic protocols for different samples where FTIR is used in terms of enhancing the everyday diagnostics and screenings for cancer.

In another review article of cancer diagnostics by Bunaciu *et al*., it was emphasized that biochemical information, objectively obtained from FTIR spectra, can be used for differentiation between cancerous and precancerous cells and tissues, with high sensitivity (55).

In a comparative study that evaluated histology and FTIR spectra of normal and tumour cells from breast, it was shown that FTIR spectroscopy is a credible method in cancer diagnostics by using the biochemical data of compounds of the respective tissue (41).

FTIR and Raman spectroscopy were used to detect tumour origin in negative lymph nodes, based on biochemical reactive changes in activated lymphocytes in early stages of disease (44).

FTIR spectroscopy was used not only for the diagnosis, but also for grading lymphomas according to the study by Andrus *et al*. (56). It was also shown to be very helpful in monitoring of treatment efficiency in colorectal cancer patients and in drug resistance research (42,56,57).

In a research done with different types of tumour cells (lymphocytes from patients with chronic lymphocytic leukaemia, tissue samples from thyroid carcinoma, and tissue samples from patients with squamous cell carcinoma), FTIR results provided the biochemical fingerprints of the particular groups of diseases that could be used for histopathological evaluation in dubious cases (46).

In another study of 43 breast samples, it was shown that alterations from normal-to-fibroadenoma, hyperplasia, ductal carcinoma in situ and invasive ductal carcinoma carry their own characteristic spectra and spectral parameters (58).

Transitional cell carcinoma can be very challenging for diagnosis because of its variety of architectural patterns, so the FTIR spectroscopy was used to identify and classify these changes and consider its role in histologically challenging cases (59).

As the matter of sample size, FTIR spectroscopy was used to differentiate endoscopic gastric samples and it was shown to have an ability to divide samples into different pathology groups like gastritis and malignancy (49).

Since the onset of its use, starting in 2004, a prostate cancer study presented improvements in optimizing procedures for using FTIR spectroscopy in diagnostics, classification and prognosis (60). In this study, advantages of infrared spectroscopy from the perspective of time and cost efficiency as well as accuracy were presented.

Also, there are some articles presenting the usefulness of FTIR spectroscopy in classification of drug efficiency in prostate cancer of different Gleason scores with sensitivity and specificity of over 92% (37,61).

An article presenting FTIR spectroscopy study of cisplatin interaction with cell components, presents promising results for using this technique for surveillance of drug interactions (62).

FTIR spectroscopy in combination with multivariate statistical analysis has been used to classify cervical precancerous lesions. Sensitivity and specificity in classifying NILM, LSIL and HSIL were above 70% and suggested that using this method as a screening tool could make a contribution in early diagnosis of cervical lesions and reduce the incidence of cervical cancer (63).

In a research in vulvar squamous cell carcinoma, FTIR spectroscopy has shown its potential to detect the genesis of malignant cells and not only the presence of cancer (64).

In a FTIR study of spermatozoa and seminal plasma, motility and concentration of spermatozoa have been analysed, and results have shown that the technique could help as a predictor of fertility (65).

Papers presented that Raman and infrared spectroscopy were used in surveillance of healing process of fractured bones, showing the influence of different treatments (66,67). Also, an article presented the results where FTIR spectra are used to see the alteration of bone molecular structure in presence of breast metastatic tumour, considering bone density, protein change and proportion of organic mass and organic matrix (68).

While ovarian cancer is usually found in late stages of the disease, the research trying to find a screening method used FTIR spectroscopy for analysing patient's blood plasma or serum for distinguishing stage I from stage II-IV disease. Sensitivity and specificity was shown to be 100% (69). Another study related to ovarian cancer used FTIR to discriminate normal, borderline and malignant tumours, guiding surgeons in right treatment (70).

The aim of this work is to use FTIR spectra for building a model which can be used to distinguish mesothelial reactive changes from malignant pleural lesions. Finding a new diagnostic method should increase the diagnostic accuracy and help avoid misdiagnosis and inadequate treatment.

1.1 Pleura

Certain organs in body cavities are covered by thin membranes, referred as the serous membranes (71). The pleura is a serous membrane that covers the lungs and lines the thoracic cavity wall (72). The parietal pleura lines the surface of the thoracic cavity and at the hilum it folds internally, making the visceral pleura, which covers the outer surface of the lung (72,73).

Hence, the parietal and visceral pleura is a continuous membrane that forms a closed cavity (7,71). This cavity, between the parietal and visceral layers of the pleura, is a real space of 10-20 microns in width (7). The thickness of pleural membrane in humans is approximately 40 microns. Histologically, pleura is lined by one layer of flat mesothelial cells, that lie on the basal membrane over a thin layer of well vascularized connective tissue. (72,74). In fact, there are five distinguished histological layers:

- One layer of flat mesothelial cells
- Basal membrane with a thin layer of underlying connective tissue
- Superficial elastic lamina
- Loose connective tissue with nerves, blood vessels and lymphatics, and
- Deep fibro-elastic tissue (73).

The amount of elastic fibers in connective tissue of parietal pleura, is lower than in visceral pleura. All histological components of the pleura are embryologically derived from mesoderm (74).

The shape of normal mesothelial cell is flat-to-low cuboidal with a width of 10 to 50 microns and height of 1 to 4 microns (71,73). By electron microscopy, the mesothelial cells

are bond to each other with desmosomes and discontinuous gap junctions, and have equal length microvilli in their apical surface (71,75). They exhibit positive immunoreactivity for high and low molecular weight keratins, Vimentin and Calretinin (74).

By means of multiple cytoplasmic pinocytic vesicles, these cells produce a clear and colorless serous liquid with protein concentration lower than 1.5 g/dL (7,72,73). Normally, there are approximately 1500 cells in one microliter of this liquid, mostly monocytes, some lymphocytes and mesothelial cells, and no erythrocytes (7). In normal conditions the volume of the liquid is 0.1 – 0.2 mL/kg of the body weight which is derived by the process of microvascular filtration (7, 71).

The role of this lubricating liquid is to smoothen the sliding movements of the pleural layers, during respiratory excursions (71,72). Gravity, together with ventilation and cardiogenic movements contribute to recirculation of pleural fluid, maintaining the equal thickness of the lubricating layer (75). Also, pleura helps in creating the positive and negative intrathoracic pressure during the ventilation cycle (73).

There is a direct communication between pleural space and the underlying lymphatic vessels, the so-called “holes” or “stomata” (76). They have a diameter of two to six microns, up to ten microns during inspiration and are found in parietal pleura (73). Different particles, such as foreign bodies or blood cells are removed from the pleural space through lymphatics through stomata (73,76).

The serous membranes of pleural cavity can be permeable to water and liquid exuded from plasma of the blood (71,72). Affected pleura in pathological conditions can allow accumulation of the liquid in this cavity called pleural effusion. Also different pathologies can cause pleural thickening.

1.1.1. Mesothelial reactive changes

Mesothelial reactive changes may occur due to inflammation, trauma, pulmonary diseases, etc.

Most of the inflammatory diseases of pleura occur due to spread from the inflammatory diseases from the adjacent lung, with resulting pleural symphysis (fusion between the two pleural layers). The subsequent fibrosis may be several centimeters thick (11,74). Pleural thickening may also result from hematoma due to an open wound of the thorax (74).

The common causes of pleuritis are: viral infections, bacterial infections, autoimmune diseases, fungal or parasitic infections, trauma, etc. (74). Tuberculosis or fungal infections can cause granulomatous inflammation, while sarcoidosis may also be a rare cause (11).

In pleural injuries, a nonspecific response called reactive eosinophilic pleuritis, which may be associated with rupture of pleural bullae in pneumothorax, may be seen (11,74).

Pleural thickening as a response to inflammation or other causes mentioned above, is a reactive change (9). In these circumstances mesothelial cells become reactive. A reactive mesothelial hyperplasia presents a reactive change of pleura due to injury of serous membrane. It may also occur in conditions such as long-standing effusions, hernias, drug reactions, trauma, surgery, inflammatory processes and tumours (11,77). In reactive mesothelial cell hyperplasia the cells tend to arrange in clusters and clumps. They become cuboidal with *"washed-out"* and vacuolated cytoplasm, indistinct cytoplasmic borders, wide separation of the nuclei, and prominent nucleoli (9,11,71). Cytological reactive atypia of mesothelial and other stromal cells, necrosis, entrapment, and papillary lumps, may resemble malignancy (9,36). Cells arranged in papillary, tubular and sheet-like structures may also be seen in inflammatory changes, as well as squamous metaplasia, mimicking epithelial type mesothelioma (36).

1.1.2. Tumours of pleura

According to World Health Organization Classification (10), tumours of the pleura are classified as the following:

1. Mesothelial Tumours,
    a. Diffuse malignant Mesothelioma
    b. Localised Mesothelioma
    c. Other tumours of mesothelial origin such as: Well Differentiated Papillary Mesothelioma and Adenomatoid Tumour
2. Lymphoproliferative disorders
3. Mesenchymal tumours.

1.1.2.1. Malignant mesothelioma

Diffuse Malignant Mesothelioma abbreviated as Mesothelioma, is the most common primary malignancy of the pleura. The cell of origin of this tumour is surface mesothelial

cell, exhibiting a diffuse pattern of infiltration over the pleural surfaces. However, there are some experimental data that the tumour cell origin is in fact sub-mesothelial stem cells that differentiate in a variety of directions (10).

1.1.2.1.1. Epidemiology

Pleural mesothelioma most frequently is seen in patients between 50 to 70 years of age, but there are occasional cases when it is also occurs in children (10,74).

Male to female ratio is 2:1 (10,11). Depending on causative factors, especially presence of the asbestos, the incidence of mesothelioma is different from country to country and has a tendency to increase (11). In North America, this ratio is 9:1 with the incidence of 2-3/million/year in women and 20/million/year in men over the last 30 years (10). There is a marked increase in incidence when asbestos exposure is combined with cigarette smoking (10,11).

The highest rates among both genders are in Australia, France, and UK. According to WHO (10), in Australia, the incidence in year 2000 was 60/million in men and 11/million in women.

In period from 1991 to 1997, in Croatia the incidence of mesothelioma was 0.8 in 100,000 (78). While in period from 2001 to 2006, the incidence was raised. There were found 342 new pleural mesothelioma cases or 1.3 cases per 100,000 population, with the highest rate shown to be in Primorsko-goranska, Split-Dalmatia and Istria County (79). According to Croatian National Cancer Registry, there were diagnosed 77 new cases in Croatia during 2015 (80).

1.1.2.1.2. Etiology and pathogenesis

More than 90% of pleural mesotheliomas in men are related to prior exposure to asbestos, also known as an occupational disease (4,10,81–83). The latency period between the onset of exposure and actual disease is 20 to 40 years (10,11,84).

Asbestos is a group of mineral silicate fibres, which based on their form, are divided into two groups, namely: serpentine (chrysolite) and amphibole (crocidolite, amosite, anthopyllite, actinolite and tremolite) (85). There are peculiar differences in affinity of types of asbestos fibres in regards to causing mesothelioma (10). Chrysotile, amosite, and

crocidolite, have different exposure-specific risks for mesothelioma in a ratio of 1:100:500, respectively, as concluded by exposure levels in professional groups (86).

Pathogenic mechanisms of asbestos carcinogeneity are not completely understood (85,87). Asbestos fibres may cause DNA damages directly by interfering mechanically with chromosomes during mitosis, and indirectly by causing mesothelial cells and macrophages to produce mutagenic reactive oxygen and nitrogen species. These oxidants may initiate activation of different signalling pathways. Mitogen activated protein kinase signalling and transcriptional activity of activator protein 1 have been associated to mesothelial cell transformation. Studies have revealed that asbestos fibres may cause inflammatory reaction with many mononuclear phagocytes, which become macrophages that phagocytize asbestos fibres and subsequently release tumour necrosis factor-α (TNF-α) and IL-1β. Additionally, asbestos induces mesothelial cells to express TNF-α receptor – TNF-R1 and to secrete TNF-α, which, when bonded to its receptor, activates the nuclear factor kappa-light-chain-enhancer of activated B cells (NF-κB) pathway for increasing the number of mesothelial cells that survive asbestos exposure. These asbestos influenced DNA damages, cause the mesothelial cells to divide and eventually, progress to mesothelioma, if this damage is genetically specific and of sufficient severity (85,87,88).

A number of fragments of inhaled asbestos fibres are deposited in the lung. Most of the fibres do not cause a tissue reaction. Some of the fibres however, may cause tissue reaction with macrophage accumulation associated with foreign body-type multinucleated giant cells. Proteins and iron derived from haemoglobin may also deposit and cause the formation of "ferruginous bodies" (10).

Asbestosis is a non-neoplastic chronic lung disease with the same etiology as mesothelioma namely, chronic exposure to asbestos fibres. It presents as a progressive pulmonary fibrosis and pleural plaques. Imaging techniques exhibit lung scarring, which together with the history of asbestos exposure confirm the diagnosis. Latency period between the onset of exposure and the actual disease is approximately 20 to 30 years. Among the symptoms of the disease are: shortness of breath, cough, clubbing of fingers, anorexia, weight loss and chest pain (89–91).

Molecular findings in mesothelioma comprise deletions of chromosome regions 1p, 3p, 9p and 6q and loss of chromosome 22 (92). These loci are suggested to be tumour suppressor genes that may play a role in the progression of malignancy. Recent research has found that some more genes are involved in carcinogenesis of mesothelioma. Mutation of BAP1 was found in mesothelioma patients, but it have been described in other cancers too

(93,94). Deletion of 9p21 which contains the CDKN2A gene, encoding a tumour suppressor p16, has started to be used as a diagnostic tool in malignant mesothelioma (93).

Studies of childhood mesothelioma do not support the connection of mesothelioma and asbestos exposure, but it cannot be completely excluded. Also, cases of non-asbestos related mesotheliomas support the idea of multifactorial etiology, starting from genetics, radiation, prenatal medication, and other possible environmental factors (95,96).

Erionite is a non-asbestos zeolite fibre, found in the region of Cappadocia, Turkey, which is another cause of malignant mesothelioma of the pleura (97). Exposure to erionite can not only cause mesothelioma, but it can also initiate interstitial fibrosis and other pulmonary changes that may affect lung function and patient survival (98), similar to asbestos.

In mesotheliomas, DNA sequences of Simian monkey virus 40 (SV40) are also found, which suggests that it may play a role in mesothelioma pathogenesis (99).

Studies showing positive family history of cancer in patients with mesothelioma, suggest a possible role of genetic factor in development of mesothelioma (99).

Rarely, mesotheliomas may appear as second malignant neoplasms. These patients underwent prior radiation for therapeutic reason, which may be causatively related to mesothelioma (100).

No specific food has been suggested as protective, but there are data that vegetable consumption may have protective effect in the development of mesothelioma, similar to the effects in other cancers (101,102).

Other causes of mesothelioma may be prior plombage therapy for tuberculosis which causes a pleural scarring (10).

1.1.2.1.3. Clinical features

Clinical features of malignant mesothelioma of the pleura are not specific. Usual symptoms are dyspnoea, cough, chest wall pain, and weight loss with anorexia (3,10). While mesothelioma is accompanied with pleural effusion in early stages, dyspnoea appears as a first symptom (103). When the effusion is drained, patients are asymptomatic, but they have continual chest discomfort (103). In recent studies, the role of malignant cells in pleural effusion in terms of studying tumour progression, cell migration and evasion from chemotherapy has been evaluated (104).

Laboratory findings in mesothelioma are anaemia, leucocytosis and thrombocytosis, sometimes associated with thromboembolic episodes and low lactate dehydrogenase (LDH) (3,11). Less common symptoms are: fever and osteoarthropathy with clubbing of the fingers. Diaphragm and vocal cord paralysis as well as nodules in the chest wall suggest progressive disease (11,105). Myalgia, dysphagia, aphonia, nausea, bad taste in the mouth, and headache, have also been reported (10,105).

High levels of hyaluronic acid in pleural fluid highly suggest pleural mesothelioma. Otherwise, lower values are a good prognostic factor (106,107).

In radiographic studies, mesothelioma may be observed as: marked pleural effusion, nodularity, pleural thickening, plaques, localized mass, and as irregular thickening of the fissures in cases where visceral pleura is involved (10,105). Invasion of the ribs may be seen in imaging studies but it is not a specific for mesothelioma (105). Asbestosis is found in very rare cases (11).

A chest computerized tomography (CT) is not an appropriate method for definitive diagnosis, but suggestive for mesothelioma if there is unilateral pleural effusion and nodular, or diffuse thickening of pleura (108). Magnetic resonance imaging (MRI) can help in differentiating invasion of the diaphragm (109). Positron emission tomography (PET) can give metabolic information, notably lymph node metastases and is more useful in staging of mesothelioma (82,110).

Each imaging modality alone, like CT, MRI and PET cannot give appropriate data for the disease. To determine the appropriate methods for diagnosing and treatment of mesothelioma, the combined use of imaging data is necessary (110).

Thoracoscopy is considered a standard procedure for obtaining tissue samples which are needed for histopathology evaluation, and macroscopic staging of the tumour spread (82).

1.1.2.1.4. Macroscopy and localization

Mesothelioma usually presents as multiple soft nodules or pleural thickening from 5-25mm, with pink, grey and yellow colour, firm to gelatinous consistency (10,11,74,105).

It is mostly found on parietal pleura, but it may also be observed in visceral pleura (10,11,74). Progression of the disease causes inosculation of the nodules resulting in fusion of parietal and visceral pleura, and lung contraction (10). This leads to chest wall pain and difficulties in ventilation.

Implantation and contiguity are usual spread patterns of malignant mesothelioma (74). Tumour spread follows the connective tissue through the interlobar fissures, diaphragm, pericardium, chest wall and even peritoneum (10,74). Inclusion of the mediastinum and contralateral pleural cavity is also seen (10). Metastases usually occur in pulmonary parenchyma, regional, axillary and cervical lymph nodes. This is not a specific finding for mesothelioma because pulmonary and other malignancies may also spread in this way (10,111). There are some reported cases of mesothelioma metastasis in skeletal muscles, endocardium and subcutaneous tissue (111), in colon found as polyp (112), brain (113), tongue (114), bone (115), and perioral tissues (116).

1.1.2.1.5. Histopathology

Diffuse Malignant Mesothelioma of the pleura is characterized by variable morphology, even in different microscopic fields of the same tumour (11). Given that mesothelium is of mesodermal origin, it is conceivable that it may be comprised of two components, namely epithelioid and sarcomatous (117).

According to WHO classification (10), mesotheliomas are divided into four histologic groups:

1) **Epithelioid mesothelioma,** is the most common histological type. It has an epithelioid cytomorphology and different morphologic patterns that may be seen in the same tumour. Tumour cells have eosinophilic cytoplasm and bland open chromatin. Mitotic figures are not frequent, except in poorly differentiated types.

Tubulo-papillary, adenomatous and solid are the most commonly found histological patterns. There are also some less commonly found patterns, like: small cell, clear cell and deciduoid types.

- Solid pattern also known as sheet-like, occurs in solid sheets, nests, or cords of round-to-polygonal cells, which have abundant cytoplasm, round, vesicular nuclei and prominent nucleoli (6). Mitoses are rarely seen in this pattern of tumour. This type of cells, and other described characteristics make this tumour very hard to differentiate from benign lesions of the pleura. Poorly differentiated patterns have discohesive round-to-polygonal malignant cells, which comes in differential diagnoses with non-Hodgkin's lymphoma and large cell carcinoma (6).

- Tubulo-papillary pattern is the most common histological epithelioid pattern diagnosed (6). It appears with tubules of different sizes, trabeculae, clefts and papillary structures with cores of connective tissue. The cells lining these forms are uniform, flat to low cuboidal, and sometimes polygonal (2,6,10). In some cases psammoma bodies are found (10).
- Microglandular pattern is often dubbed as adenomatoid. It appears with gland-like and micro-cystic structures lined by flat-to-cuboidal cells. It may predominate in the same tumour, but often it is found with other patterns of mesothelioma. It usually comes in differential diagnosis with metastatic adenocarcinoma of the lung (6,10).
- Small cell pattern is very rarely found. Tumour cells are small, round with bland nuclei and high nucleus-to-cytoplasm ratio. It should be differentiated from metastatic small cell carcinomas from other sites, primitive neuroectodermal tumour (PNET) and lymphoma (6).
- Clear cell pattern is characterized by tumour cells with clear cytoplasm. This type of cells makes this tumour resemble other clear cell tumours that may be metastatic to the pleura, from other origins. This type usually occurs in combination with other histological patterns of mesothelioma, so this may be of helpful discriminating feature (10).
- Pleomorphic pattern is described to contain anaplastic and/or tumour giant cells (10).
- Deciduoid pattern is characterized with proliferation of round-to-polygonal cells, with eosinophilic cytoplasm, round vesicular nuclei with prominent nucleoli, resembling decidual cells of pregnancy. This pattern is very rarely predominant, but it may be found focally with other histologic patterns within epithelioid group (6,118).

According to research done by Mašić et al, epithelioid mesothelioma samples were classified in solid (26.4%), tubulopapillary (25.3%), trabecular (24.2%), tubular (11%), adenomatoid (2.2%), microcystic (2.2%), micropapillary (2.2%), acinar (1.1%) and pleomorphic (1.1%) subtypes (119).

2) **Sarcomatoid mesothelioma**, is a type of mesothelioma characterized by spindle cells arranged in fascicles or in haphazard distribution (6,10). Atypia, necroses and mitotic activity are more conspicuous in this pattern. It may resemble fibrosarcoma, but it also may contain anaplastic and giant multinucleated tumour cells mimicking malignant fibrous histiocytoma (MFH). Foci of osteosarcoma and chondrosarcoma may rarely be seen in this histological pattern (6,10).

- Lympho-histiocytoid foci may rarely occur in this pattern, with malignant histiocytoid appearing mesothelial cells admixed with marked lymphoplasmacytic infiltrate (120). Histiocytoid-like tumour cells and vast numbers of inflammatory cells may lead to erroneous diagnosis of inflammatory non neoplastic lesion. Non-Hodgkin's and Hodgkin's lymphoma may also be considered in the differential diagnosis (6).

3) **Desmoplastic mesothelioma,** may occur as a sarcomatoid and epithelioid variant, but usually is of mesenchymal appearance. It is characterized by atypical spindle cells set in ample amounts of disorganized or storiform collagen. Areas of typical sarcomatoid mesothelioma may be seen throughout different areas of the tumor.

4) **Biphasic mesothelioma**, is a mesothelioma that consists of both patterns namely, sarcomatoid and epithelioid, in at least 10% of the tumour tissue. It may present as a combination of any histologic pattern within the epithelioid and sarcomatoid types. Approximately 30% of all mesotheliomas are of biphasic type (6,10).

Pleomorphic and transitional patterns are also described as tumours that do not have the characteristics of any histological patterns mentioned above. Giant and/or anaplastic cells, respectively with hybrid epithelial and sarcomatous features in the same tumor cell are seen (6).

Diffuse malignant mesothelioma and localised malignant mesothelioma have different clinical behaviours hence, it is very important to differentiate one from the other (10).

1.1.2.1.6. Spread and staging

Malignant Mesothelioma of pleura usually gives metastasis in nearby organs like regional lymph nodes, lung, liver, adrenals and kidneys (112). It is not usual to have distant metastasis of mesothelioma, but there are some rare reported cases, like multiple metastasis in multiple skeletal muscles, endocardium and skin, together (111). Also, rare cases of tongue metastasis (114), and metastasis presented in bleeding colonic polyp, were reported two years after treatment and negative follow up (112).

Metastases of mesothelioma are rarely seen in intracranial space, but rare cases of brain metastasis near the subarachnoid hemorrhage hematoma resection were reported (113).

Since 1967, there have been many struggles for staging of malignant mesothelioma, proposing five systems (121). International Mesothelioma Interest Group presented a staging system, but because of some irrelevant issues, TNM classification based in surgical-pathological features remains the staging system proposed by the International Mesothelioma

panel and UICC (Union for International Cancer Control) (10,108,121). Last updated TNM staging exceeds restrictions in metastasis descriptors (122,123). The classification system is based on three elements:

- T summarizes the spread of the main tumour,
- N summarizes the spread of the cancer to regional lymph nodes,
- M signifies the presence of metastases to other organs,

According to Brigham system (124), which is destined to be used for qualifying patients for surgery, there are four stages of pleural mesothelioma:

Stage 1 - tumour involves only parietal pleura (1A) or involves two pleural layers (1B),

Stage 2 - tumour has spread to the chest wall and lungs, but still is present only in one side,

Stage 3 - tumour is still present in one side but has metastasized to lymph nodes and may be spread to alongside organs,

Stage 4 - tumour has spread to other side and organs of the thorax, diaphragm, peritoneum and distant organs.

1.1.2.1.7. Treatment

If the tumour is discovered in early stages and treated with extra-pleural pneumonectomy followed by chemotherapy and radiation therapy, it is thought that disease can be cured (10).

According to the Guidelines of the American Society of Clinical Oncology and ESMO Clinical Guidelines for diagnosis, treatment and follow up, there are three methods used for treatment of mesothelioma: surgical methods, radiotherapy and chemotherapy. Surgical treatment performed in mesothelioma cases can be as radical pleurectomy and decortication (125,126). Patients with disease in early stages should have radical surgery combined with chemotherapy and/or radiation therapy (125,126)

Radiotherapy should be performed at palliative and symptomatic disease patients (125,126).

Chemotherapy is recommended in patients with mesothelioma, because it of improving survival and life quality (125,126).

Everyday novelties in cancer genesis and diagnostics of malignant mesothelioma, give options for individual therapy in different patients. As a new promising target may be BAP1 (127). Having in mind that hypoxia helps in development of aggressiveness in

tumours, control measure of hypoxia in tumour such as mesothelioma may be therapeutic strategy (128).

1.1.2.1.8. Prognosis

Even though there are data that each histological pattern has its prognostic behaviour, still mesothelioma remains a tumour with poor prognosis.

The average of survival for untreated patients is around six to twelve months (10,129). In some studies there are data that age, sex, geographic area, and tumour stage are important prognostic factors (10,108). Older male patients, non epithelioid histological subtype, low haemoglobin, low LDH, anaemia, high leucocyte and thrombocyte level, chest pain, dyspnoea, weight loss, are associated with poorer prognosis (108,121,129).

Tumoral CD10 expression was presented to be related with aggressive histologic types, mitotic activity and an independent prognostic factor in malignant mesothelioma patients (130).

It was shown that patients with mesothelioma that have loss of BAP1 protein, have seven times better prognosis than others (131,132).

1.1.3. Metastatic tumours to pleura

The pleural cavity shows to be tempting metastatic site for malignant tumours from nearby organs and distant organs, too (133). Metastatic pleural tumours present about 75% of the tumours of the pleura (74). Cancer cells are transferred to the pleura through vascular or lymphatic system and body fluids, usually causing pleural effusion that presents an advanced stage of disease (134).

Mostly found metastatic tumours in pleura are lung cancer, breast cancer, lymphomas, genitourinary, and gastrointestinal tract tumours (133,135).

The most likely histological type of cancer that metastasizes in pleura is adenocarcinoma of the lung, and since it is located nearby, it may spread by contiguity and has the tendency to invade the vasculature (7).

Both, visceral and parietal pleura may be affected by the metastatic tumours that usually cause pleural effusion. Some of the symptoms are similar as those encountered in primary tumours of pleura, like dyspnoea, cough, and weight loss.

1.1.3.1. Lung tumours

The most frequent and one of the most deadly cancer types is lung cancer, which in men is mostly associated with smoking (10).

According to WHO, lung tumours are classified in: 1. Epithelial tumours, 2. Mesenchymal tumours, 3. Lymphohistiocytic tumours, 4. Tumours of ectopic origin and 5. Metastatic tumours.

Epithelial lung tumours are classified as follows: a) adenocarcinoma, b) squamous cell carcinoma, c) neuroendocrine tumors, d) large cell carcinoma, e) adenosquamous carcinoma, f) sarcomatoid carcinoma, g) other and unclassified carcinomas, h) salivary gland-type tumours, i) papillomas and j) adenomas (10).

1.1.3.1.1. Lung adenocarcinoma

The most common differential diagnosis dilemma in routine practice is between epithelioid MPM and adenocarcinoma of the lung metastatic to pleura. Lung adenocarcinoma is a malignant epithelial tumour that shows glandular differentiation, produces mucin, with acinar, papillary, micropapillary or solid growth patterns and express either mucine or pneumocite marker (10).

While adenocarcinoma of the lung is located in the periphery, and based in data from different diagnostic methods, the idea that the cell of its origin are pneumocites type II and Clara cells, is supported (10).

1.1.3.1.1.1. Etiology and epidemiology

Tobacco smoking is strongly related factor with adenocarcinoma in men, while it is also seen in women that never smoked (10,136).

Adenocarcinoma is less seen in men (but has a tendency to rise) than in women, where it is the dominant histological type of lung cancer, except for women in Poland, England, and Scotland, where predominant are other lung cancer types (10).

There are reflections in incidence and mortality form lung cancer related with dose, duration and type of tobacco.

1.1.3.1.1.2. Clinical features

Clinical features are progressive shortness of breath, cough, chest pain/ oppression, hoarseness or loss of voice and rarely haemoptysis. Recidivism of pneumonia sometimes is the leading property in many patients. Most often patients with lung adenocarcinoma are asymptomatic till the late disease course (11).

In radiographic studies, lung adenocarcinoma is seen as peripheral nodular formation under 4 cm in diameter, while chest wall and pleura invasion is seen in about 15% of cases.

A chest computerized tomography (CT) has shown characteristics that can distinct adenocarcinoma from other histological types of lung cancer. Known patterns of adenocarcinoma by CT imaging are solid nodules, ground glass opacities and mixed opacities (137).

Again, thoracoscopy should be performed for ensuring tissue samples needed for histopathological evaluation, and macroscopic staging of the tumour spread (82).

1.1.3.1.1.3. Macroscopy, localisation and histopathology

Lung adenocarcinoma is found as single or multiple nodules of different sizes (136). There are six macroscopic patterns found, sometimes combined, having corresponding radiological correlates: peripheral tumour, central (endobronchial) tumour, diffuse pneumonia-like, diffuse bilateral, pseudo-mesotheliomatous and tumour in underlying fibrosis (10,136).

Isolated histological patterns of lung adenocarcinoma are: lepidic, acinar, papillary, micropapillary, solid, and variants of lung adenocarcinoma are also invasive mucinous, colloid, fetal, enteric, minimally invasive and preinvasive lesions (WHO, 2015) (10). According to WHO tumour classification (10), mixed subtype is most usual tumour composed of the histological patterns described below:

- The lepidic adenocarcinoma is characterised with bland pneumocites (type II pneumocites or Clara cells) growing through pre-existing alveolar structures with present invasion component.
- The acinar pattern is described with glandular structures built from columnar or cuboidal tumour cells that may produce mucin.

- The papillary pattern tumour replaces the pre-existing lung architecture with papillae that have secondary and tertiary papillary structures, built with tumour glandular cells throughout fibrovascular cores.
- The micropapillary carcinoma pattern characterized with papillary structures forming florets but do not have fibrovascular cores.
- Solid adenocarcinoma is characterized with sheets of polygonal tumour cells with mucin present in some tumour cells.
- Invasive mucinous adenocarcinoma was found to be mixed invasive mucinous and mucinous type.
- Minimally invasive adenocarcinoma can be of mucinous and non-mucinous type.
- In preinvasive lesions are included atypical adenomatous hyperplasia and adenocarcinoma in situ (mucinous and non-mucinous).

1.1.3.1.1.4. Spread and staging

Lung adenocarcinoma spreads usually by lymphatic and haematogenous ways, but aerogenous propagation is also noticed, especially in bronchoalveolar/lepidic pattern adenocarcinoma (10,138). Adenocarcinomas located peripherally often involve pleura imitating malignant mesothelioma, especially in small biopsies and radiologically (10).
Metastatic lung adenocarcinoma most frequently is seen in organs such as brain, adrenals and liver (138).

1.2 Diagnostic methods

Histopathology remains the main method for diagnosing different lesions. There are some other methods that help in diagnostic accuracy, but still histopathological opinion gives way to other researches.

1.2.1. Immunohistochemistry

Immunohistochemistry is a method that uses immunologic abilities to identify cellular and tissue molecules (74). Its principles are based in antigen-antibody reaction. IHC also plays an important role in prognosis prediction and also in treatment planning (136).

Even though there are many immunohistochemical markers found until today, which are used to enhance the diagnostic accuracy, differential diagnosis in pleural lesions still remains a diagnostic challenge, because even immunohistochemistry has its limitations. There are immunophenotypic overlapings found among mesothelioma and its mimics (139). Many studies dealing with diagnosis of pleural lesions with immunohistochemical analysis show that sensitivity and specificity of single antibodies are not satisfied, which is the reason for using antibody panels for achieving higher diagnostic accuracy (135). Immunohistochemical markers should be estimated depending on the histological subtype of mesothelioma (140). Antibody panel used for differentiating mesothelial origin of the tumour most of the times shows positivity in reactive mesothelium.

Standard immunohistochemical panel includes Calretinin, Cytokeratin 5/6, WT-1, D2-40 and possibly other markers such as CEA, CAM 5.2, Thrombomodulin, TTF-1, panCytokeratin, CD44H, LeuM1, EMA, p53, MOC-31, Ber-Ep4, CD147, HBME-1, E-cadherin, BG-8, MOC-1, B72.3, claudins (1, 2, 3, 4, 5, 7) (10,12–15,141,142).

Calretinin is very useful antibody used in standard immunohistochemical panel. Its expression indicates mesothelial origin of the tumour. Calretinin is positive in epithelioid mesotheliomas and majority of sarcomatoid mesotheliomas, but it shows expression also in some adenocarcinomas, squamous cell carcinomas, sarcomatoid carcinomas and sarcomas (13,17,135,143).

Many studies trying to elect the most useful immunohistochemical panel include Cytokeratin 5, which is very sensitive positive marker in mesothelioma (18,140,143–146). It shows expression also in some lung adenocarcinomas, serous carcinomas and lung squamous carcinomas (143,146).

WT-1 was shown to be also very useful in differential diagnosis between epithelioid and sarcomatoid mesothelioma with lung adenocarcinoma, with its positivity from 75 - 99% of epithelioid type mesotheliomas, while it shows reactivity in up to 15% of adenocarcinomas (16,77,143,146). WT-1 together with CAM5.2 was shown to be very sensitive and specific in differentiating sarcomatoid mesothelioma from sarcomas (143).

Thrombomodulin in many studies was found to be a sensitive mesothelioma marker and less specific, and in that way becoming a good additional marker in immunohistochemical panel for differential diagnosis between mesothelioma and metastatic lung adenocarcinoma in several cases (15,20,139,140,147).

HBME-1 was also shown to be high specific and lower sensitive marker in differentiating mesothelioma from metastatic lung adenocarcinoma, and can enhance accuracy in diagnosis of these tumours (8,14,18,135).

Immunohistochemical markers such as CD44H, N-cadherin, podoplanin, mesothelin, in many studies, somewhere less and somewhere more in percentage, have shown to be positive in mesotheliomas, and in that way help in diagnostic accuracy in differential diagnosis between these tumours (17,77,146). Their expression was found also in other tumours, that makes them less specific in diagnosis, but knowing that every case should be treated as individual, they can give their help in final diagnosis.

In sarcomatoid type mesothelioma, positive markers are shown to be Calretinin, Thrombomodulin, D2-40, WT1, CAM5.2, AE1/AE3 and CK7 (77,139,143).

Diagnosis of mesothelioma should also take into consideration at least two negative markers (135).

TTF-1 has shown to be very useful negative marker for mesothelioma in differential diagnosis between adenocarcinoma. In many studies, TTF-1 was 100% negative for mesothelioma, and excluded its diagnosis, but recently a case has been reported with malignant mesothelioma TTF-1 with positive reaction (10,16,18,20,77,144,146,148,149).

CEA, CD15, Ber-EP4, B72.3, MOC-31, BG8, Leu-M1, E-cadherin are also suggested to be very helpful negative markers in differential diagnosis between mesothelioma and adenocarcinoma (14–17,20,77).

Ki67 as nuclear protein is used as a proliferation marker and was shown contradictory results in differentiation of mesothelial reactive changes and malignant mesothelioma in pleural effusions (150,151). In another study it was shown that Ki67 can be used as a prognostic marker for epithelioid type of malignant mesothelioma, but not in non-epithelioid subtypes too (152).

To date, the number of antibodies available to help in differential diagnosis is every day growing, but their usefulness remains controversial and there is no immunohistochemical marker completely sensitive and specific for differentiating mesothelioma from its simulators (135). The number of antibodies that should be used is not specified, but there could be used two mesothelial markers and two markers for the tumour in differential diagnosis, for

example adenocarcinoma, sarcoma or other, but if still doubts, then add other helpful markers. Loss of BAP-1 by imunnohistochemistry is found only in mesothelioma, but not in all of them (77).

1.2.2. Electron microscopy

It has proven to be very credible method in diagnosis of malignant mesothelioma. Its role in this purpose is limited because diagnostic ultra-structural features described are seen only in epithelioid type mesotheliomas, it is much more expensive and slow than immunohistochemistry, and it is not helpful at all at not differentiated mesotheliomas (14,15,77).

1.2.3. Vibrational spectroscopy

Seeing the need and the importance for finding an objective method in differential diagnosis, our idea evaluates vibrational spectroscopy as an analytical method and a new diagnostic tool in pleural pathology.

Vibrational spectroscopy is one of the oldest analytical and research method, which studies the interaction of the electromagnetic waves and matter. There are two types of vibrational spectroscopy - infrared and Raman, whose main difference lies in the type of vibrations and transitions that are being measured. Although both techniques were previously used to analyze pathological samples (153), hereafter we will limit our discussion to infrared spectroscopy.

Infrared spectroscopy involves the interaction of infrared radiation with matter and is nowadays routinely used to obtain spectra from different types of samples such as liquids, solids, gases, slurries and suspensions (1,154). Based on light absorption, transmittance or reflection, this method helps in identifying the molecular nature of samples. The principle of infrared spectroscopy is based on the fact that almost all molecules absorb infrared radiation (46). Energies of the vibrational modes of molecules in the samples are of the same order of magnitude with the energies of infrared radiation hence irradiating the samples with infrared radiation is accompanied with the excitation of vibrational modes of molecules. Every bond whose vibration changes the molecule’s dipole moment has the potential to contribute to an infrared spectrum. Mid-infrared (mid-IR) spectral region with wavenumbers from 4000 to

400 cm^{-1}, is the main region of vibrational spectroscopy and holds the majority of information for identification of organic molecules (41).

Different tissues, cells, or fluids have different percentage of various molecules and consequently different biochemical content. For that reason they will have different reaction to infrared radiation and obtained infrared spectra will also be different. While human cells are composed of water, proteins, nucleic acids, lipids and carbohydrates, pathological changes in the body leading to diseases are thought to be due to some biochemical changes in one or more than one of these components. If vibrational spectra are sensitive to the structure of these components, then they must change with the diseased state (1). The different infrared spectra are the information we can use to distinguish between normal or abnormal cells and tissues (154). In other words, the different cells, or even different development states of a cell, create a different infrared spectrum, identifying either their type or their state based on different biochemistry of their compounds (41).

In 1950, for the first time the protein conformation studied by IR spectroscopy was demonstrated (154). The development of high performance Fourier transform infrared (FTIR) spectrometer was the key of eventual using of IR spectroscopy in biology (1,154). FTIR, with name originating from mathematical process of Fourier transform used to convert the raw data ('interferogram') into the actual spectrum, is a powerful technique in which FTIR spectrometer simultaneously collects data over a wide spectral range, thus offering a significant advantage (e.g. Fellgett advantage, Jacquinot advantage, Connes advantage etc.) over a previously used dispersive spectrometers. Recently it was shown that tumor cells can be distinguished from their normal counterparts by observation of their FTIR spectra (37–39). Hence, vibrational spectroscopy can be considered as a new diagnostic tool. Having in mind that vibrational spectroscopy can be used to analyze different kinds of samples, it holds significant promise for analysis of pathological samples.

2. HYPOTHESIS

Vibrational spectra of normal pleura, pleura with inflammatory changes, with primary neoplastic disease, and with metastatic disease, will be different and in this, constitute a potentially useful tool in the differential diagnosis of pleural pathology.

3. AIMS OF THE STUDY

3.1. GENERAL AIM

Correlation between morphological entities and vibrational spectra achieved with vibrational spectroscopy.

3.2. SPECIFIC AIMS

Comparison of vibrational spectra of normal pleura, pleura with inflammatory changes, pleura with primary neoplastic disease and metastatic disease. Possible application of the vibrational spectroscopy as an additional tool in differential diagnosis of pleural lesions.

4. MATERIALS AND METHODS

4.1 Tissue samples

In our study, we compared the vibrational spectra of tissue samples from 32 patients with different pathologies, to see if there are some differences in FTIR spectra. Tissue samples of pleural malignant mesothelioma, pleuritis and metastatic lung adenocarcinoma in pleura were obtained from the paraffin blocks retrieved from the archives of the Department of Pathology, University of Zagreb - School of Medicine. While samples of normal pleura were prepared in that way that we took fresh lungs from autopsy cases, peeled pure pleura and put it in paraffin blocks. All samples were taken from different patients respectively.

Table 1. Types and number of tissue samples

Tissue type	Number of patients	Number of sections / patient	Sections for histopathology evaluation (5 μm)	Samples for vibrational spectroscopy – FTIR (10 μm)
Normal pleura	2	22	4	40
Inflammation	10	23	2	210
Mesothelioma	10	23	2	210
Adenocarcinoma	10	23	2	210

From each tissue block, 23 new tissue sections were cut and prepared. The first and the last section were 5 microns thick, while the 21 others were 10 microns thick. The first and the last section were stained with Hematoxylin & Eosin (HE) and re-examined by a pathologist using optical microscope in order to ascertain the type of tissue.

The 21 tissue sections from each block became 21 samples for FTIR spectroscopy. One spectrum was recorded from each of 690 samples, from each tissue block (patient) with mesothelioma, inflammation and metastatic adenocarcinoma were prepared 21 samples and from two blocks of pleura we prepared 20 samples (table 1). First, samples for FTIR spectroscopy went through the deparaffinization process. Paraffin was removed following standard histology protocols; 21 new tissue sections from each block were put on optical

grade silicon windows (background) and placed in thermostat for one hour, than they were placed in three xylene troughs for 10 minutes each. At the end, samples were placed in vacuum for 60 minutes to extract remaining water. Optical grade silicon window is transparent to IR radiation and it is used very often as an infrared substrate for different samples. In this way, prepared samples (Figure 1) went to spectrometer for recording spectra (lasting 5 minutes for each section). Each tissue section presents one sample for FTIR recording.

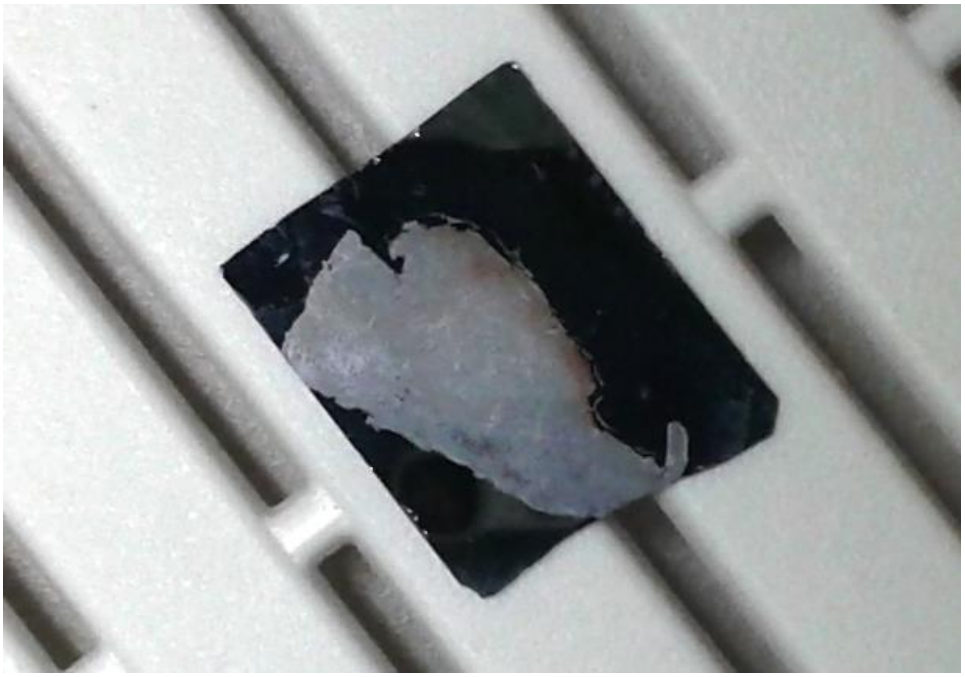

Figure 1. Tissue sample in optical grade silicon windows

4.2 FTIR spectroscopy

FTIR spectrometers are composed of three elements: internal IR light source, interferometer and a detector which is connected to an amplifier and computer. Vibrational spectra of our samples were recorded with PERKIN-Elmer SPECTRUM GX spectrometer equipped with liquid N_2 – refrigerated Mercury Cadmium Telluride (MCT) detector. IR light source used was voltage-stabilized, air-cooled coiled wire operating at 1350 K. An interferometer, which modulates the infrared beam, consisted of a moving and fixed mirrors, and a beamsplitter. The beamsplitter divides the beam in two and the moving mirror creates an optical path difference between them, thus creating an interference pattern (interferogram) which is measured and analysed (Figure 2).

Optical grade silicon windows were used for acquiring 1000 scan background, which was automatically subtracted from tissue spectra. Such a large number of background scans was indispensable for the improvement of the signal-to-noise ratio and correct elimination of the atmospheric absorption (i.e. oxygen and carbon-dioxide absorption). 100 scans were performed for each tissue section in order to obtain the vibrational spectra, which lasted around 5 minutes for each sample. Data were acquired in 4000 – 450 cm^{-1} spectral range, in transmission mode with a resolution of 4 cm^{-1}.

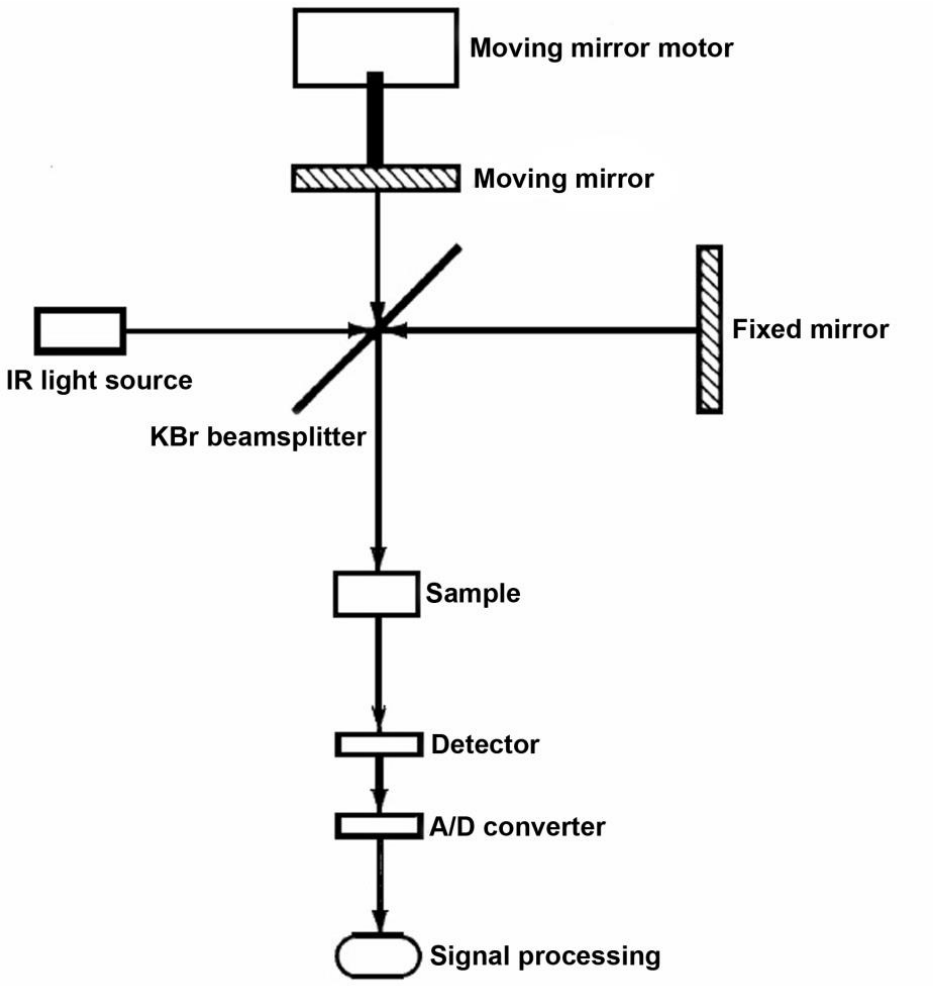

Figure 2. FTIR spectrometer scheme (155)

4.4 Data analysis

The specific software called Kinetics (42), running under Matlab 7 (Mathworks), was used for processing the spectra. First, all recorded spectra were baseline corrected and normalized by the same procedure. Baseline correction and normalization are relevant preprocessing techniques for FTIR spectra. Preprocessing creates a linear correlation between absorbance and concentration. Many physical and chemical factors can affect this correlation like: sample size, humidity, interferents, molecular interactions, etc. The preprocessing techniques compensate the deviations from linear relationships and intensify the relationship between the spectral signals and concentrations of the analytes. Preprocessing corrections lead to the slight changes of raw spectra. Baseline correction was done in the same manner in all spectra. Baseline of the spectra was determined by the lowest characteristic points along the spectrum (156).

The Matlab and PLS Toolbox (Eigenvector Research) were used to obtain the principal component analysis (PCA). PCA can be used to detect differences between the spectra. Data from the recorded spectra are processed with PCA statistical analysis. PCA is a variable compression method that reduces the data set of matrix to a much smaller number of variables called principal components. Usually, only the first two principal components, PC1 and PC2, which account for most of the variance presented in the experimental data, are utilized in majority of applications, although in some cases even higher-order components hold relevant data. PCA is a method used to reduce the data matrix into a simpler one whereas deleting worthless information from the spectra. Using PCA a quantitative model was made, which can be used to determine unknown samples in the future. Based on the created model, new undetermined samples can be added and their possible belonging to a certain group can be established.

Another statistical method, used to evaluate differences between different groups, was Student's t-test. Student's t-test is a statistical method that makes possible to compare two means, by telling if they are different and if the differences are significant. To provide the difference spectra, the mean spectra of one group of samples were subtracted from the mean spectra of another group, in six combinations. Student's t-test was used for analysing the provided difference spectra in the manner that each wavenumber was examined to determine if the difference in intensity between mean spectra of two tissues is statistically significant. STT is applied for each wavenumber in the spectrum, which means that for a single wave number the values of intensity and all observed spectra are taken (for example:

mesothelioma, metastasis). This means that using STT, the statistical significance of differences is calculated in mean spectra of the certain group of samples, in six different combinations. Each difference spectra gained in six combinations (shown in pictures bellow) presents calculated difference from the mean spectra of certain sample combination, indicating in which part of the spectra the differences exist.

5. RESULTS

5.1 Histopathological evaluation

In our samples selected from the archive, the original histopathological diagnoses were based on morphology and immunohistochemical (IHC) analysis. In order to assure tumour tissue quality by microscopic observation, the first and the last section of all selected paraffin blocks were stained with HE and reviewed by a pathologist.

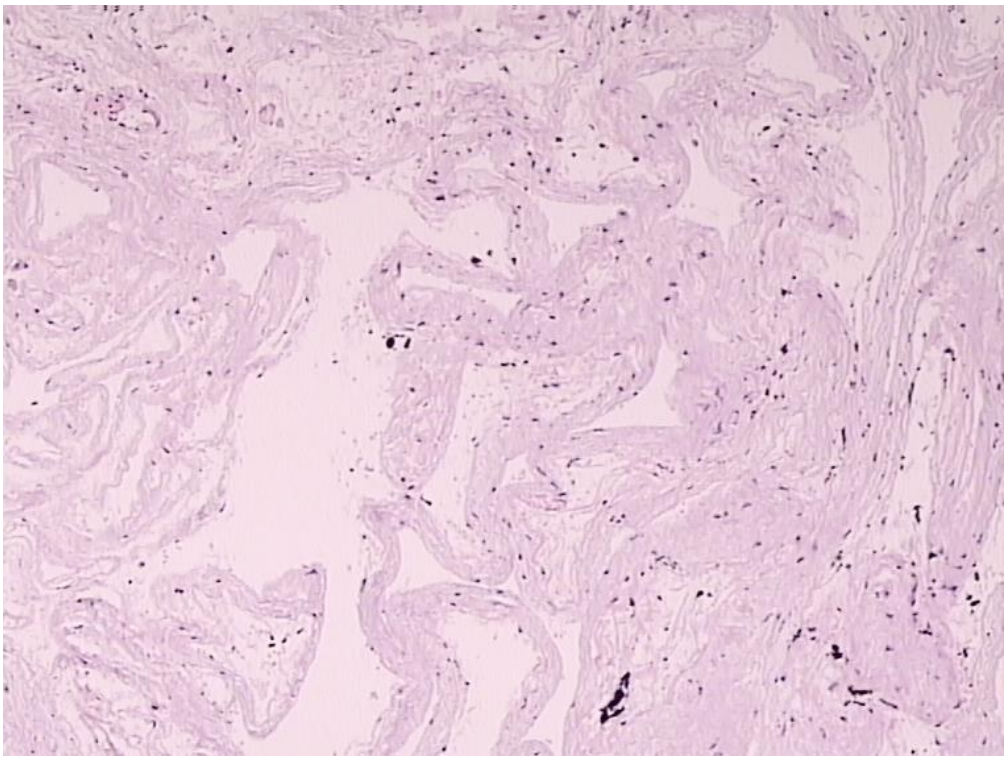

Figure 3. Normal pleura (HE staining at magnification of 20x)

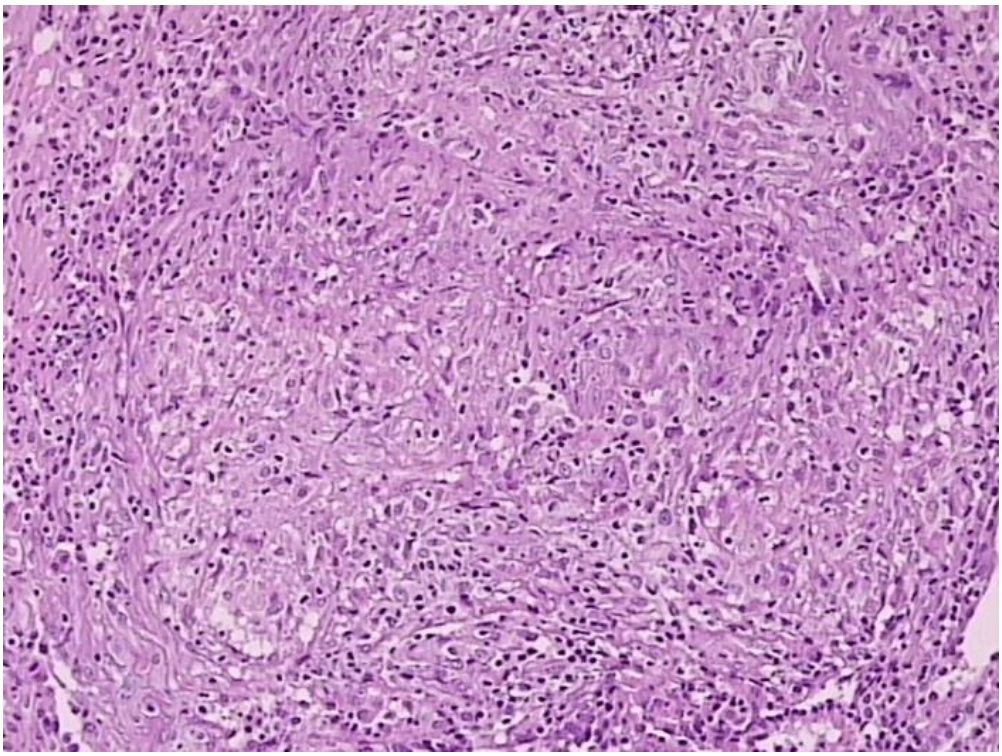

Figure 4a. Reactive mesothelial changes due to inflammation (HE staining at magnification of 20x)

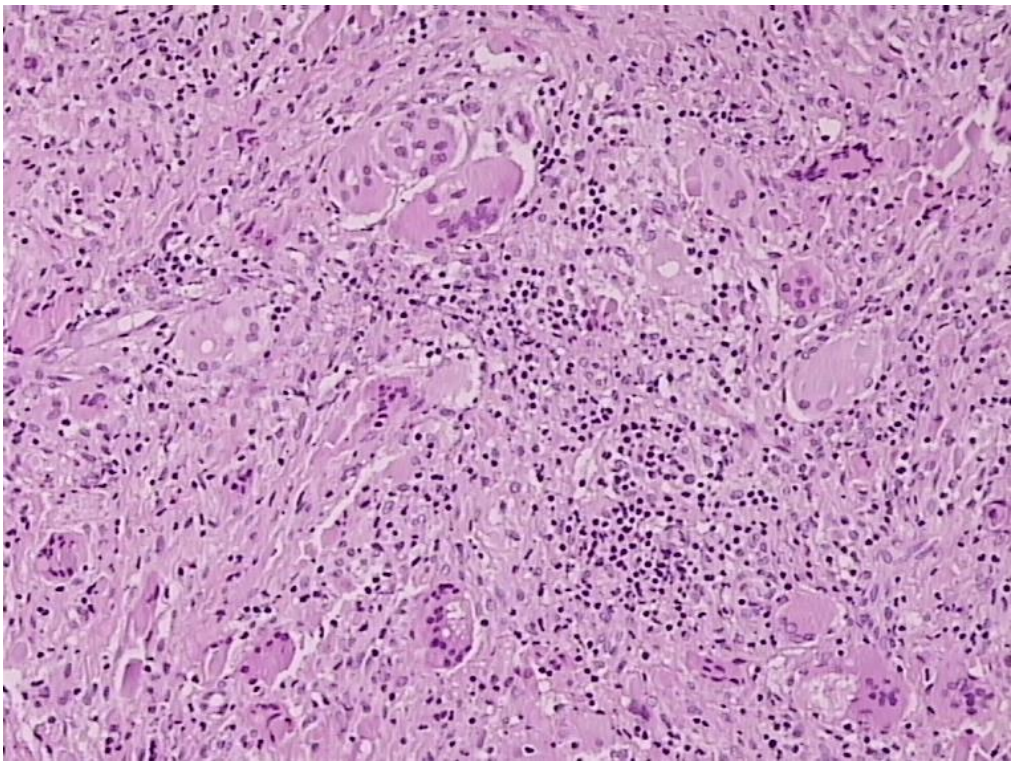

Figure 4b. Reactive mesothelial changes due to granulomatous inflammation with giant cells (HE staining at magnification of 20x)

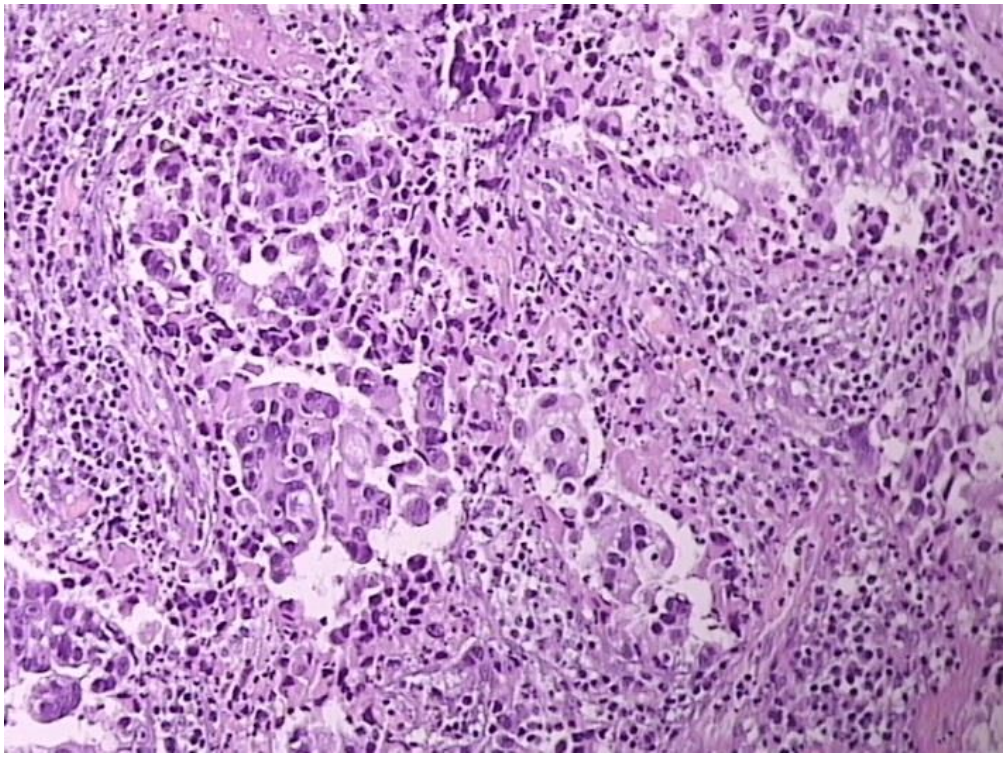

Figure 5a. Metastatic lung adenocarcinoma, in pleura (HE staining at magnification of 20x)

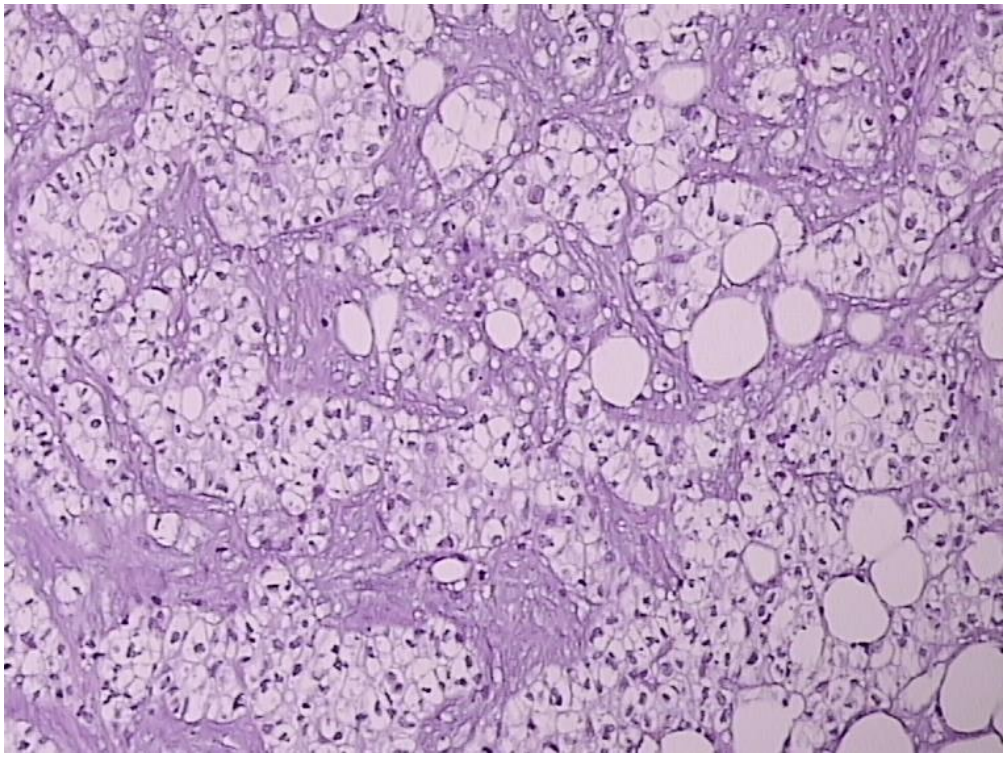

Figure 5b. Metastatic adenocarcinoma (clear cell) in pleura (HE staining at magnification of 20x)

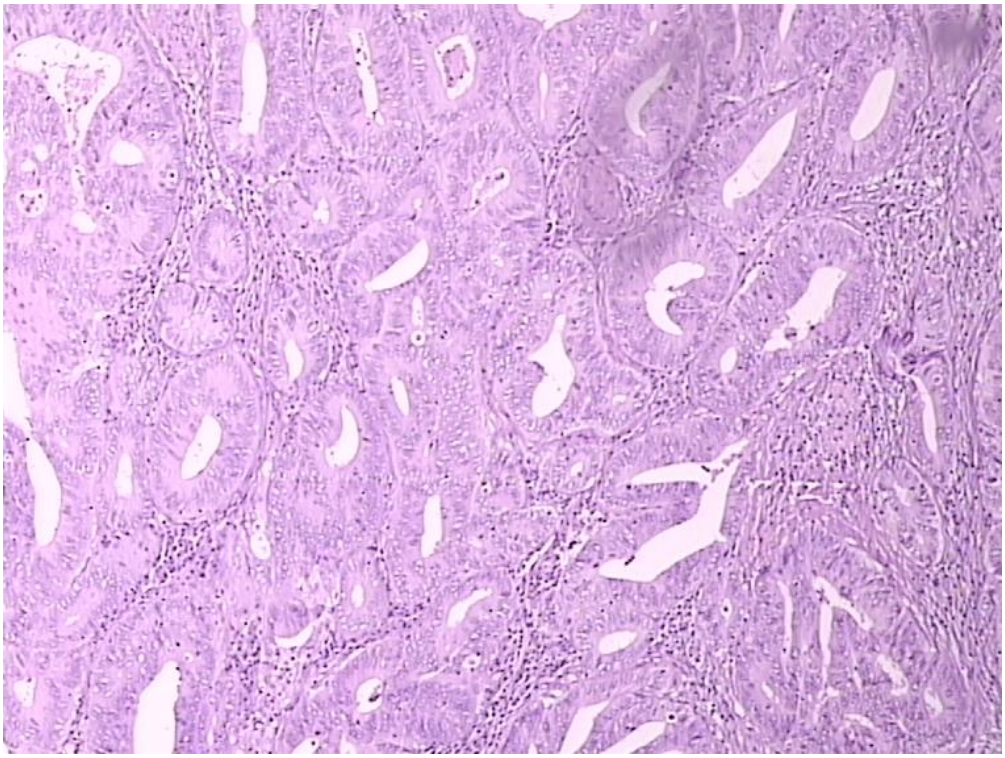

Figure 5c. Metastatic adenocarcinoma (from colon) in pleura (HE staining at magnification of 20x)

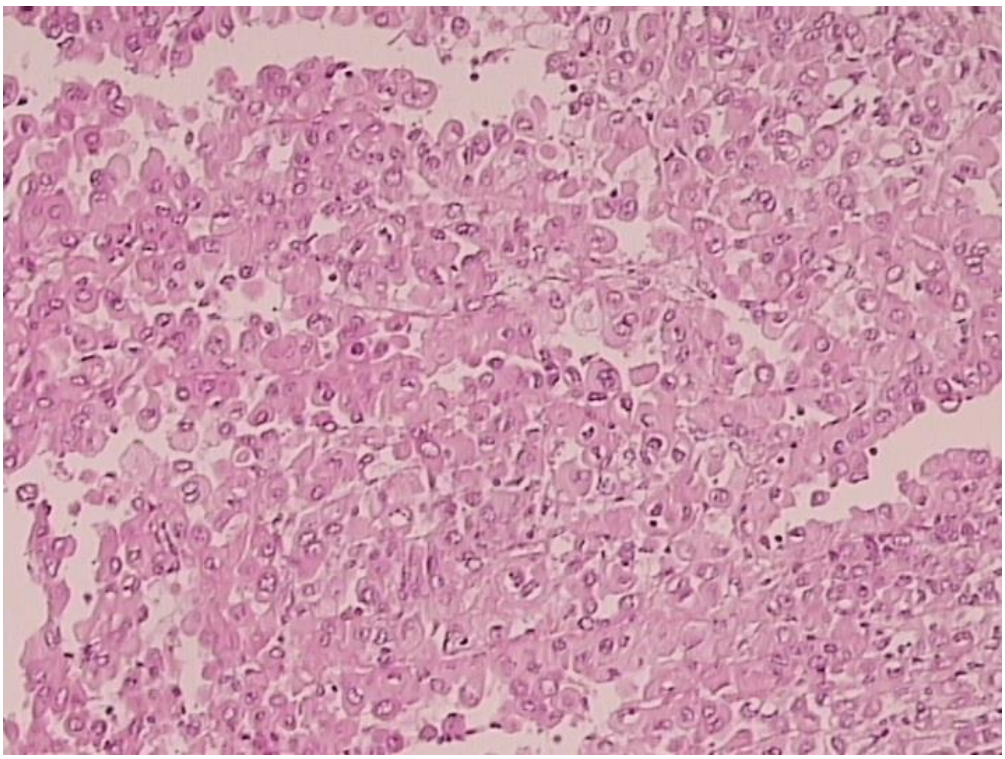

Figure 6a. Mesothelioma – epythelioid type (HE staining at magnification of 20x)

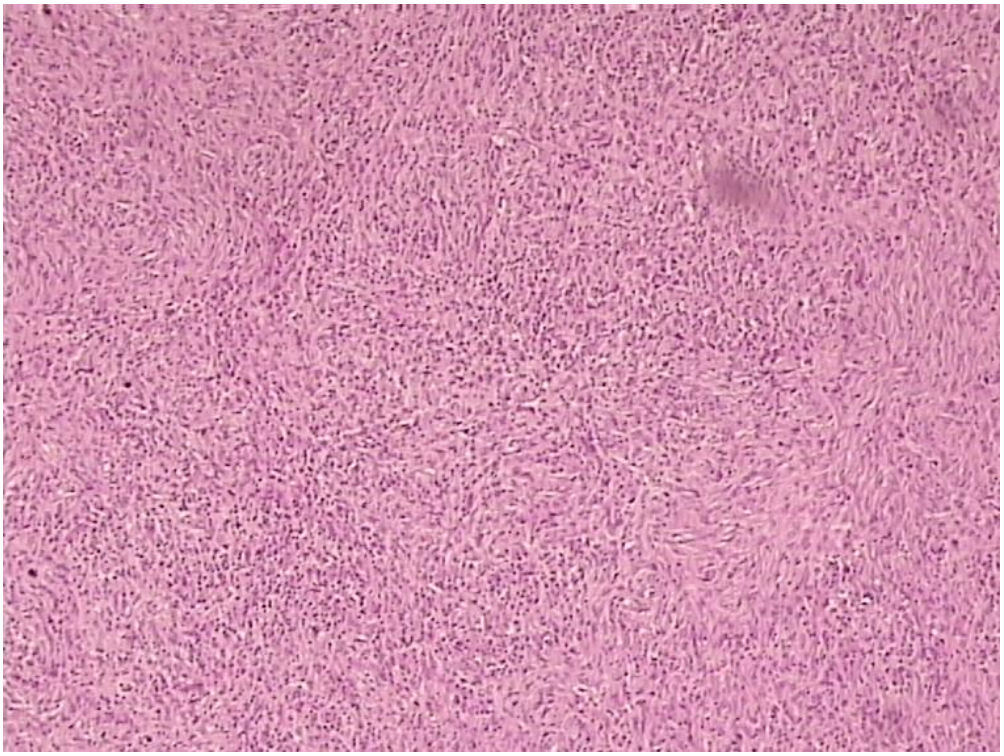

Figure 6b. Mesothelioma – sarcomatoid type (HE staining at magnification of 20x)

Normal pleural tissue samples were from visceral pleura, without lung tissue and prepared in a swiss role fashion (as seen in figure 3).

In our study, all inflammatory diseases of pleura samples were chronic inflammations (Figure 4a) including 4 samples of granulomatous pleuritis with giant cells (Figure 4b).

Metastatic adenocarcinoma in pleura (Figure 5) samples originated from lungs (seven samples) (Figure 5a), kidney - clear cell (two samples) (Figure 5b), and colon (one sample) (Figure 5c).

The studied malignant mesothelioma of the pleura samples consist of 6 epithelioid type (Figure 6a), 3 sarcomatoid type (Figure 6b) and one biphasic type.

Table 2. Histopathology diagnosis and number of cases

Histopathology diagnosis			
Normal pleura	2		
Pleura inflammation (10)	Chronic inflammation 6	Granulomatous pleuritis 4	
Mesothelioma (10)	Epithelioid 6	Sarcomatoid 3	Biphasic 1
Metastatic adenocarcinoma (10)	From lung 7	From colon 1	Clear cell type 2

5.2 FTIR spectra

Mean spectrum of all recorded spectra from each type of tissue is shown (Fig. 7). All spectra of the same tissue group were collected into one mean spectrum, with variations in intensity covered by noise and differences created due to recording conditions. They are all baseline corrected. Significant differences between spectra are in the peaks with wavenumbers shown in Table 3.

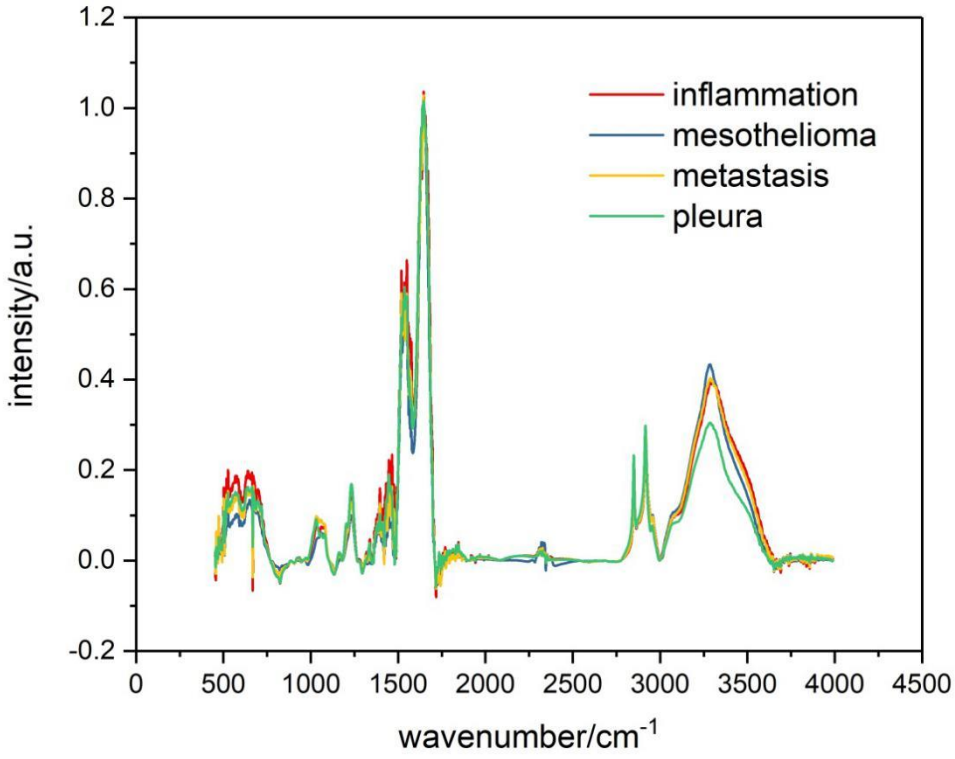

Figure 7. Mean value of spectra from four groups of samples. Blue line presents inflammation; Red line - mesothelioma; Green - metastasis; Purple - pleura.

Every mean spectrum in figure 7 was calculated by collecting all the spectral numbers and divided by the number of spectra from the respective group of samples.

Table 3. Band assignments of wavenumbers where we found significant differences in FTIR spectra of mesothelioma, metastatic adenocarcinoma in pleura, pleuritis and normal pleura (based on literature (40,157,158)).

Wavenumber (cm^{-1})	Definition of the spectral assignment
3611	O-H & N-H stretching vibrations
3500 - 3600	OH bonds
3500 - 2800	Cholesterol, phospholipids and creatine (higher in normal tissues) Stretching vibrations of CH2 & CH 3 of phospholipids, cholesterol and creatine

3401	O-H &N-H stretching vibrations
3396	O-H asymmetric stretching
3330	N-H asymmetric stretching
3300	Amide A bands sterning from N-H stretching modes in proteins and acid nucleic
3008	Olefinic – CH stretching vibration: unsaturated lipids, cholesterol esters
3000 - 2800	C-H, lipid region, CH3,CH2-lipid and protein
2870	CH_2 symmetric stretching: protein side chains, lipids, with some contribution from carbohydrates and nucleic acids
2851	CH_2 symmetric stretching: mainly lipids, with the little contribution from proteins, carbohydrates, nucleic acids
2600	H-bonded NH vibration band
2100	A combination of hindered rotation and O-H bending (water)
2000 - 1500	Fundamental stretching vibrations of double bonds (e.g. C=O, C=C, C=N)
1740	Ester C=O stretch: triglycerides, cholesterol esters
1468	CH_2 scissoring: lipids
1453	CH_2 bending: mainly lipids with the little contribution from proteins
1400	COO^-symmetric stretching: fatty acids
1343	CH_2 wagging: phospholipid fatty acid, triglyceride, amino acid side chains
1238	PO_2^-asymmetric stretching fully hydrogen – bonded: mainly nucleic acids with the little contribution from phospholipids
968	C-N^{+-}-C stretch: nucleic acids, ribose-phosphate main chain vibrations of RNA – DNA
915	Ribose ring vibrations: RNA/DNA
868	Left-handed helix DNA (Z form)

The infrared spectra of the studied tissues is complex, consisting of many spectral bands due to the presence of macromolecules (lipids, proteins, polysaccharides, and nucleic acids). The tissues absorb the infrared beams in spectral regions: 800 to 1800 cm^{-1} and 2800 to 3700 cm^{-1}.

The diameter of infrared light beam that passed through the tissue sample was 1 cm which means that we recorded spectrum from everything that was in the field of 1 cm diameter of every sample. As tumour samples are heterogeneous in their composition (159–161), every compound of every sample gave its contribution to the recorded spectra, leading to the final result of recognising the difference between different pathology and separating samples into discrete groups.

5.3 Student's T-Test

In the next step we continued our analysis with Student's T-Test. This test was used to statistically significant differences of spectra at corresponding wavenumbers. Student's T-test (STT) was performed on all six possible pairs of mean spectra of different tissue types: metastasis – mesothelioma, metastasis – inflammation, metastasis – pleura, mesothelioma – inflammation, mesothelioma – pleura, and inflammation – pleura. Student's T-test was calculated for every wave number with significance level of $p<0.01$. Thicker parts of lines in differential spectrum (red lines) show wave numbers with significant difference.

Student`s T-test can only be performed on pairs of tissue samples. So, on the figures bellow are presented Student`s T-test performed on compared pairs. In every Student`s T-test, blue and green lines present the mean spectra of compared groups, while the red line presents differential spectrum of the compared group.

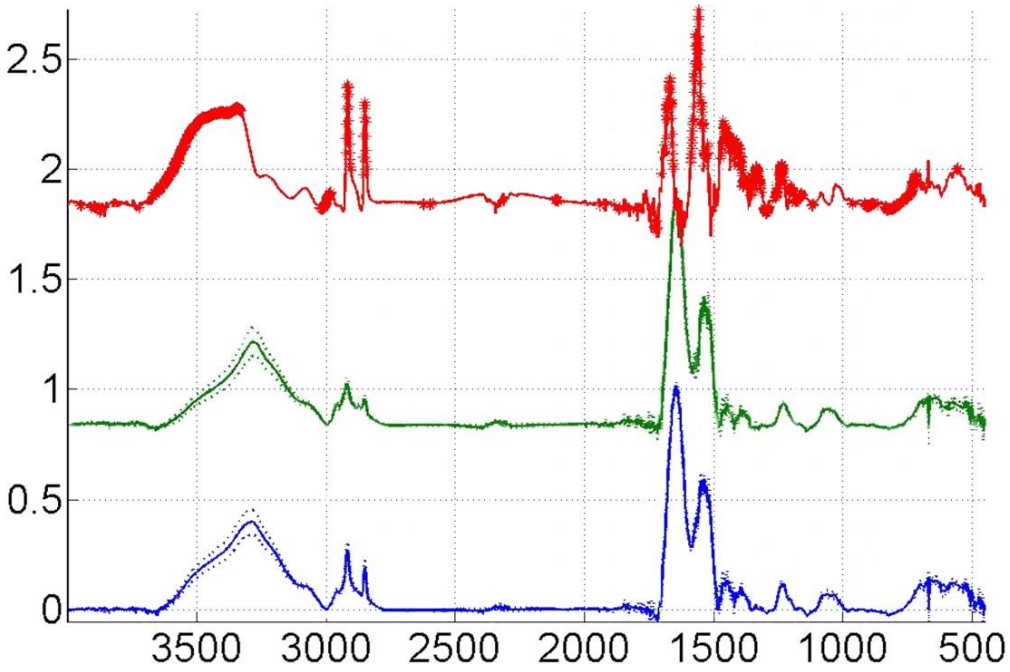

Figure 8. Student's t-test for every wave number, on combination: metastasis (blue line) and mesothelioma samples (green line). Red line is the differential spectrum between these two groups.

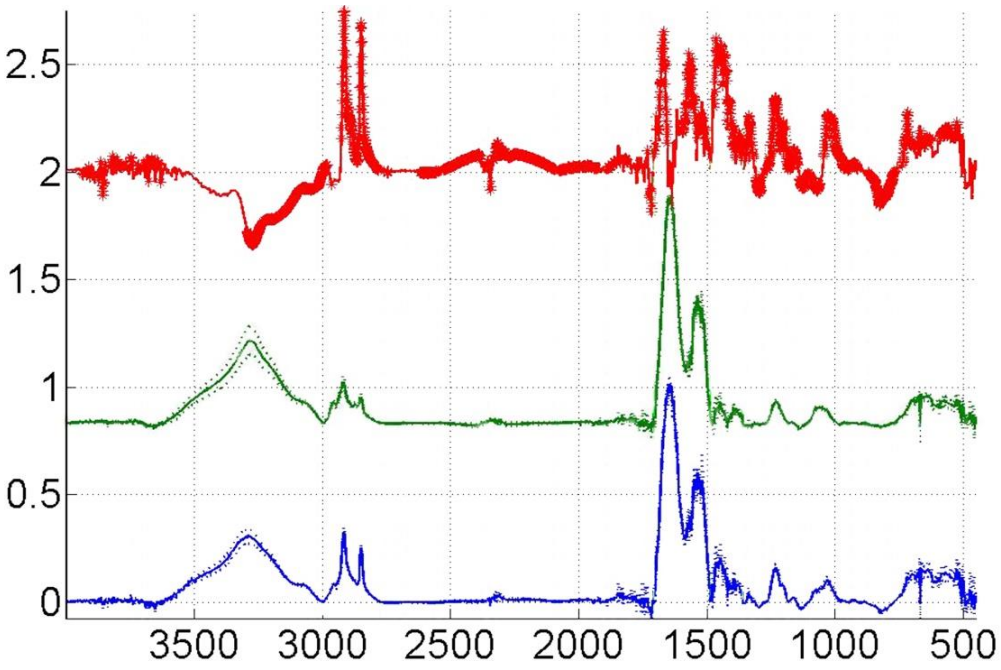

Figure 9. Student's t-test for every wave number, on combination: pleura (blue line) and mesothelioma samples (green line). Red line is the differential spectrum between these two groups.

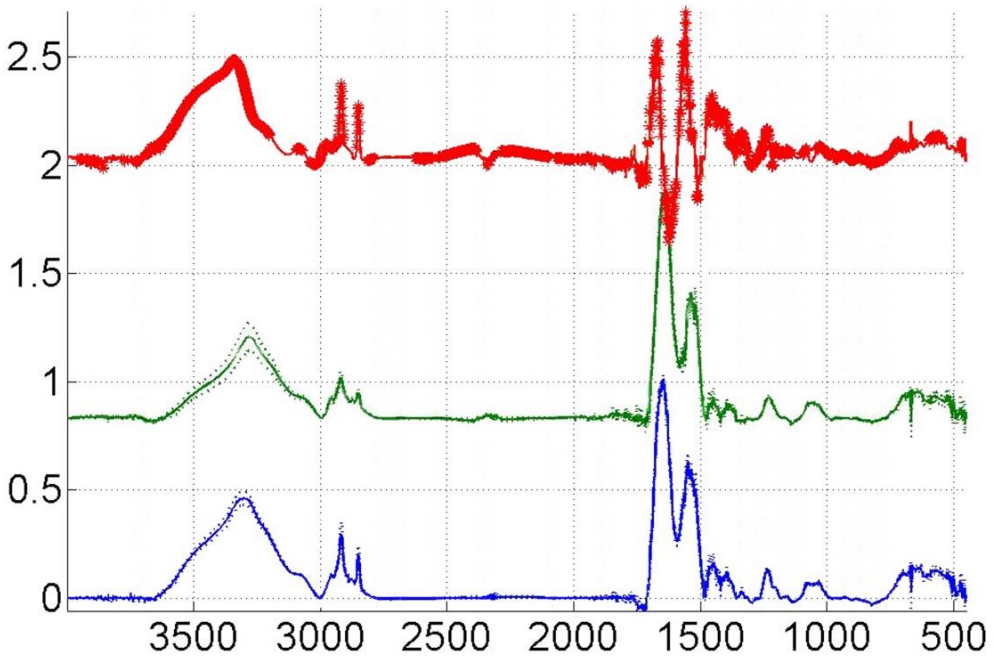

Figure 10. Student's t-test for every wave number, on combination: inflammation (blue line) and mesothelioma samples (green line). Red line is the differential spectrum between these two groups.

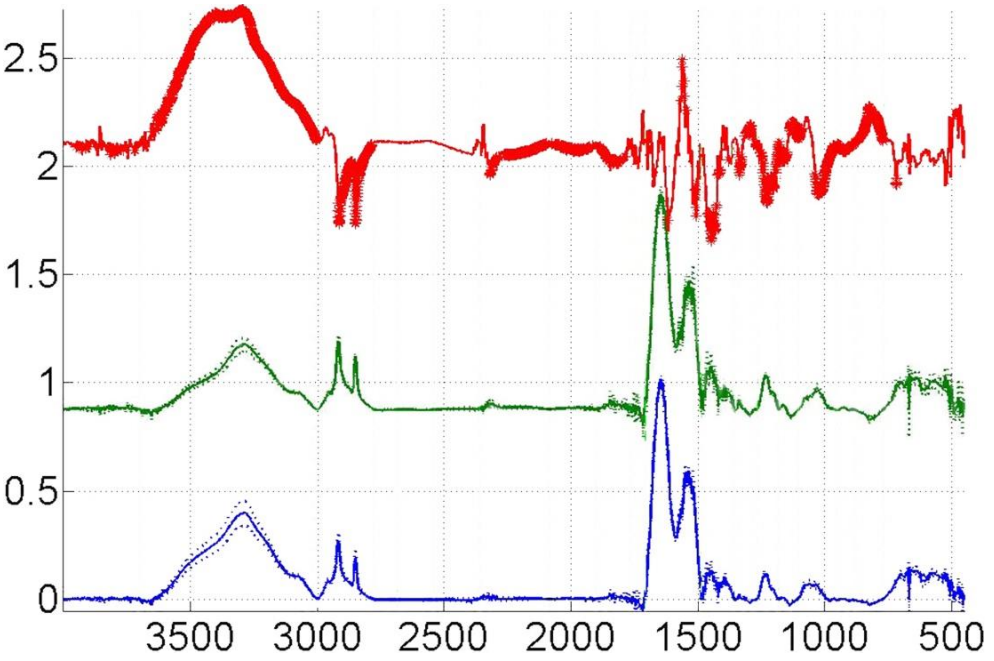

Figure 11. Student's t-test for every wave number, on combination: metastasis (blue line) and pleura samples (green line). Red line is the differential spectrum between these two groups.

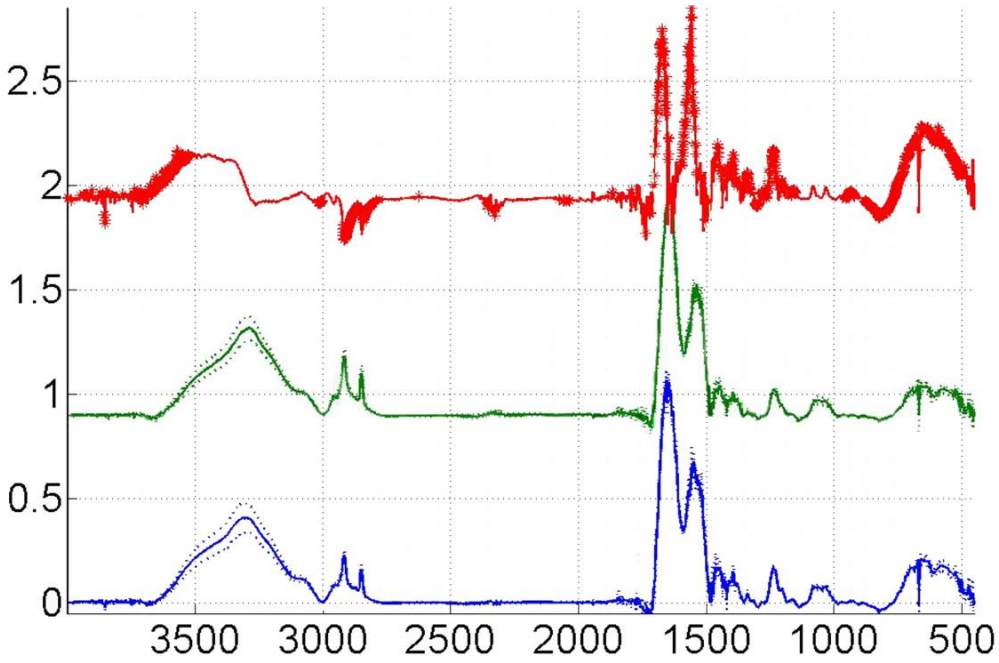

Figure 12. Student's t-test for every wave number, on combination: inflammation (blue line) and metastasis samples (green line). Red line is the differential spectrum between these two groups.

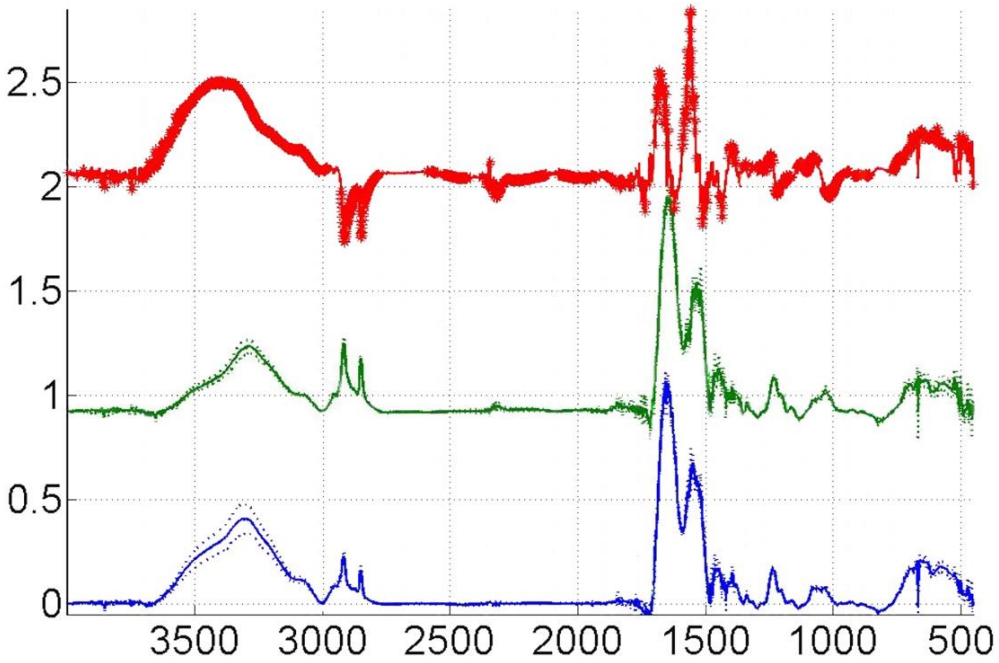

Figure 13. Student's t-test for every wave number, on combination: inflammation (blue line) and pleura samples (green line). Red line is the differential spectrum between these two groups.

Student T-test indicated the differences between the spectra of different pathologies, so we decided to generate PCA model. Changes in the spectra, detected by the student T-test, verify the differences in intensity between different pleural tissue. So the idea was to generate PCA model with hope that differences calculated with STT will help to identify pathology of the unknown samples.

Based in the spectral differences observed by STT, PCA model presented below could identify the different pathologies. Differences exist between spectra and they are used by the model to assort unknown tissue samples into a pathological category. Differences in intensity and location are placing different samples into a certain group of pathology in our model (Figure 21).

5.4 Principal Component Analysis

Observed differences in intensity, band width and position of the vibrational band between spectra, shown in Figures 8, 9, 10, 11, 12 and 13, indicate that it is possible to build a PCA model from recorded spectra, which might be able to distinguish between three investigated pathological tissue types and may identify spectra of the samples with unknown pathologies. FTIR spectra of biological samples are often very similar and important differences are covered with noise and spectral changes caused with small but unavoidable sample preparation variations. Therefore, statistical analysis must be used to recognize spectral changes due to the treatment or disease.

Before statistical analysis, the mean centre pre-processing was applied on all spectra. Also, all spectra were baseline corrected and normalized before analysis. Figure 14 shows the scatter plot of PCA scores for the two first principal components of four groups of recorded spectra: mesothelioma, metastatic lung adenocarcinoma in pleura, pleuritis and normal pleura.

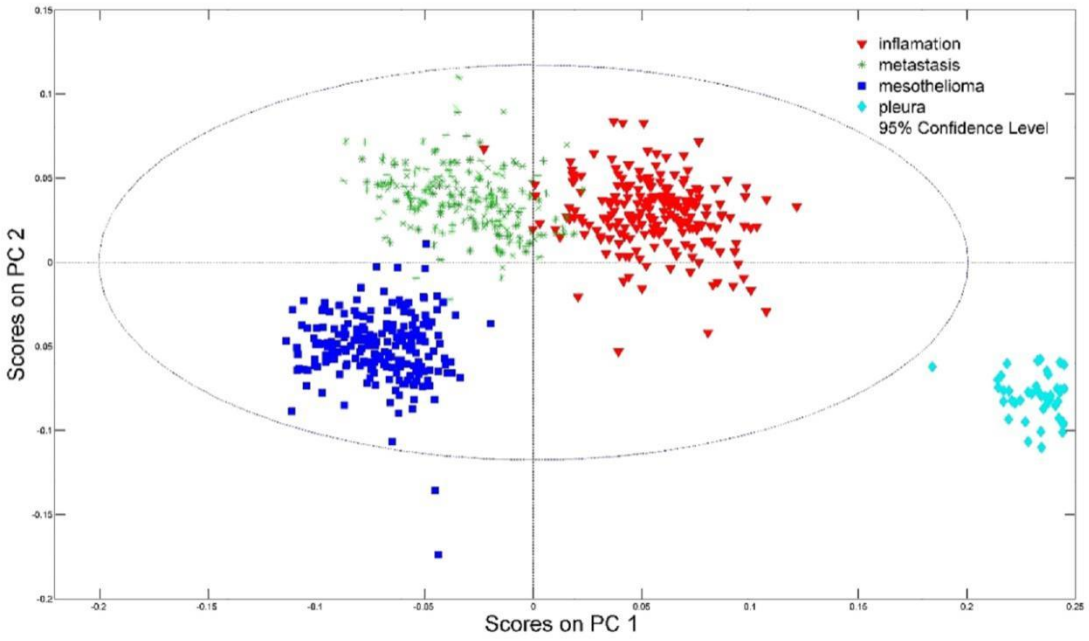

Figure 14. PCA statistical analysis of all recorded spectra. Blue squares represent spectra of the mesothelioma, green stars represent the spectra of metastases, red triangles are spectra of inflammation and light blue rhombuses are spectra of normal pleuras.

As seen in Figure 14, it is possible to distinguish between four groups of tissues. In the principal components PC1-PC2 space, there is a difference between FTIR spectra recorded from samples of mesothelioma, metastatic adenocarcinoma in pleura, inflammatory and normal pleura. Although there is not a clear distinction between the mean spectra of four groups of samples plotted in Figure 8, 9, 10, 11, 12 and 13, the difference is visible after application of PCA in Figure 14. Few spectra that overlap or fall into proximity of other groups do not change successfulness of presented PCA model. Reasons for overlapping spectra between two different tissue groups are probably small differences in recording conditions or sampling procedure. Nevertheless, their number is small and can be excluded from the model without further consequences in the model precision. Number of problematic spectra can also be reduced by more precise defining of sample preparation and spectra recording procedure.

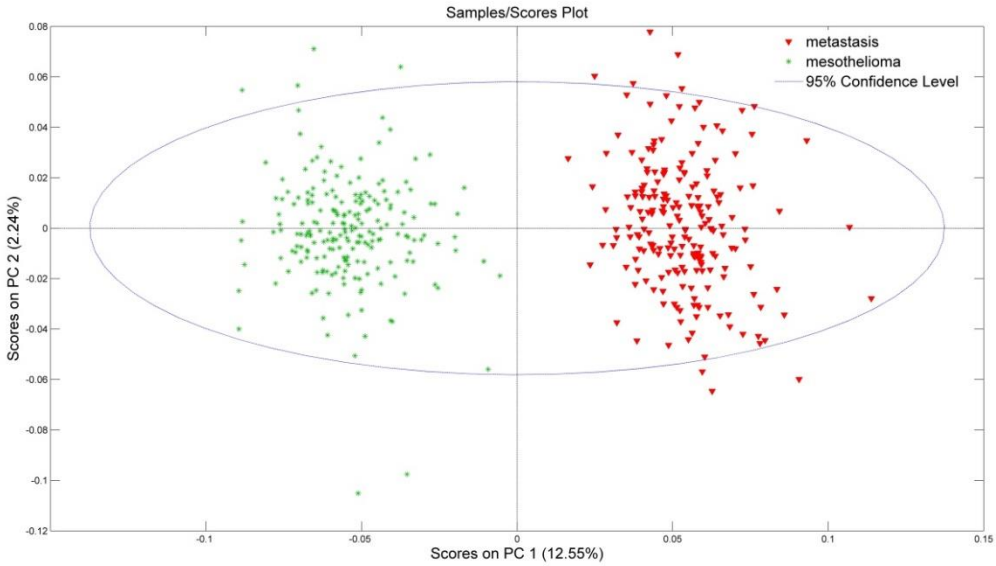

Figure 15. PCA statistical analysis of mesothelioma and metastasis spectra. Green stars represent spectra of the mesothelioma, red triangles are spectra of inflammation.

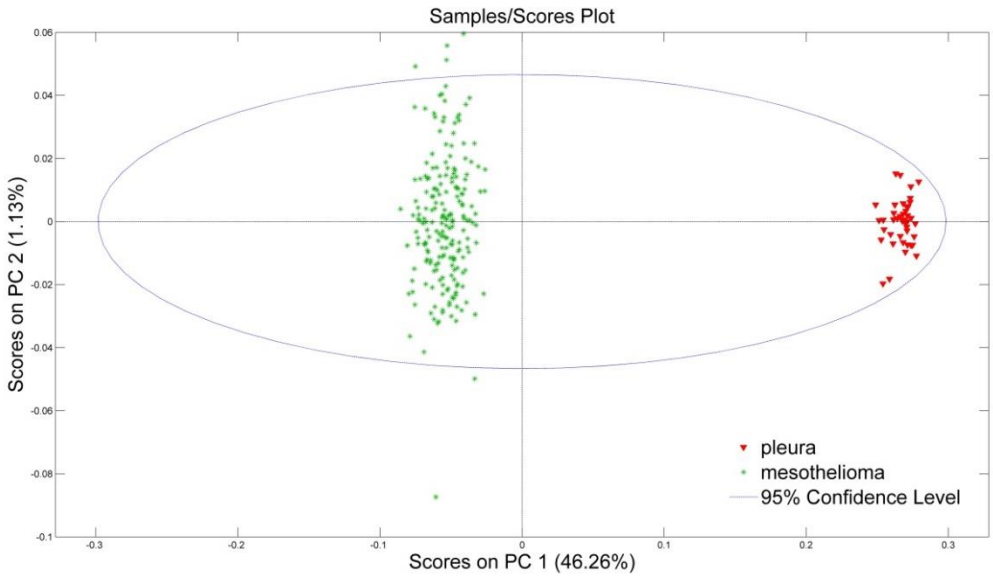

Figure 16. PCA statistical analysis of mesothelioma and pleura. Green stars present spectra of the mesothelioma, red triangles are spectra of inflammation.

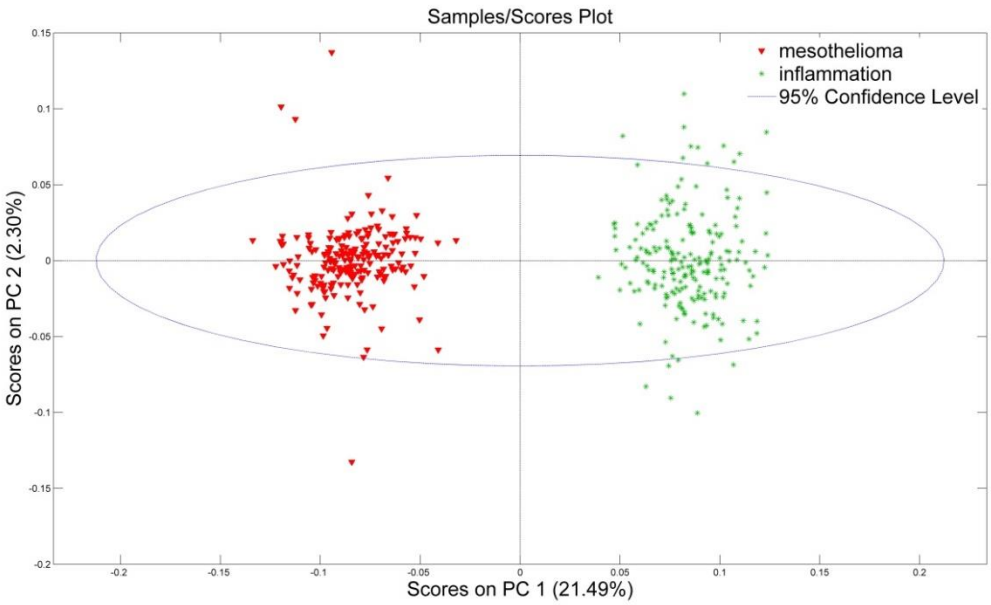

Figure 17. PCA statistical analysis of mesothelioma and inflammation. Red triangles are spectra of mesothelioma and green stars represent the spectra of inflammation.

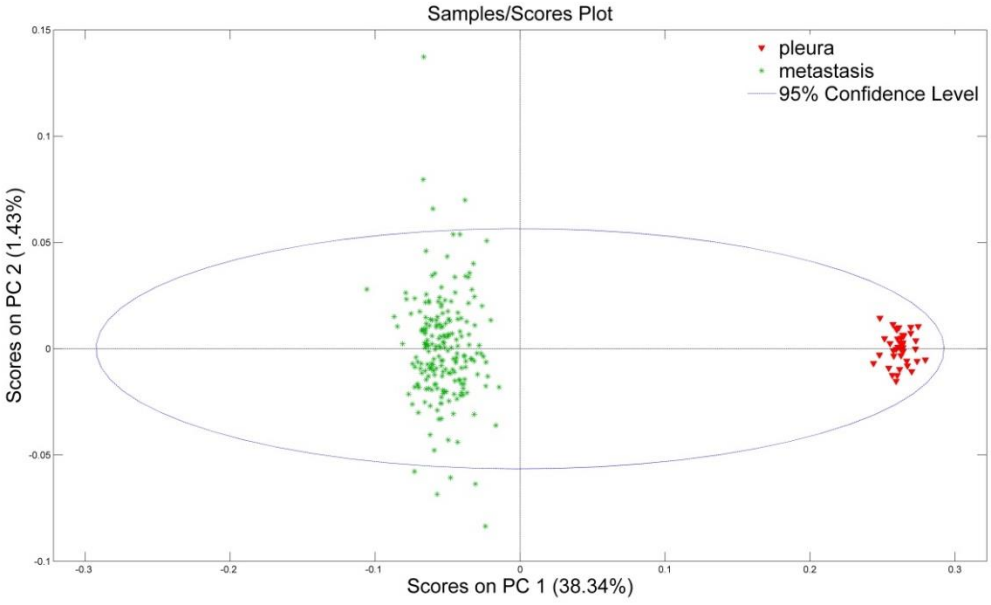

Figure 18. PCA statistical analysis of all metastasis and pleura recorded spectra. Green stars represent the spectra of metastases and red triangles are spectra of normal pleuras.

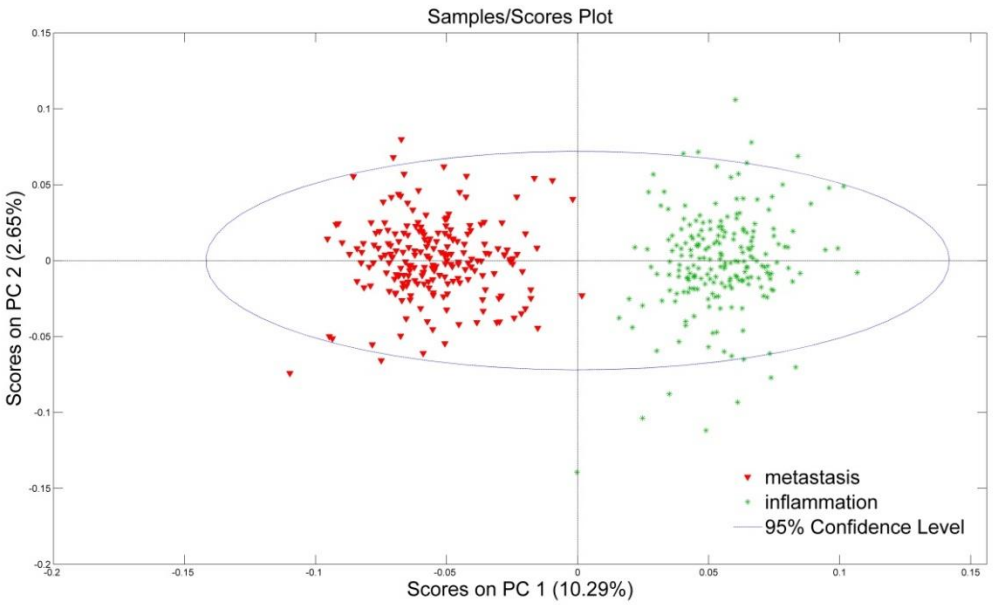

Figure 19. PCA statistical analysis of all metastasis and inflammation recorded spectra. Green stars represent the spectra of metastases and red triangles are spectra of inflammation.

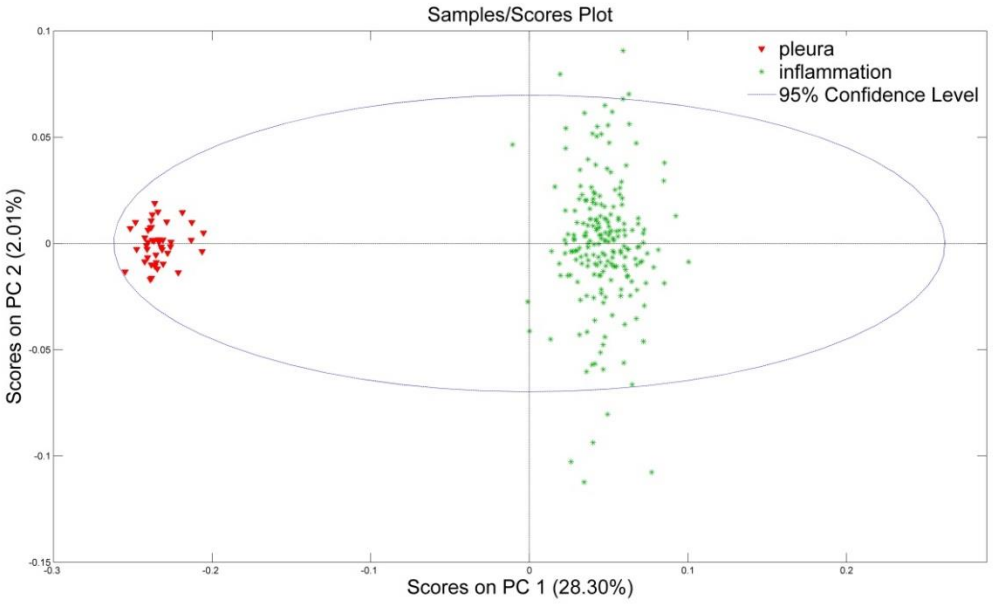

Figure 20. PCA statistical analysis of all pleura and inflammation recorded spectra. Red triangles are spectra of normal pleura and green stars represent the spectra of inflammation.

PCA statistical analysis was generated for groups consisting of pairs (same groups as in STT: metastasis-mesothelioma, mesothelioma-pleura, mesothelioma-inflammation, metastasis-pleura, metastasis-inflammation, pleura-inflammation). Figures of the PCA above (Figure 15, 16, 17, 18, 19 and 20) show that in the principal components PC1-PC2 space for every compared group there is a difference between FTIR spectra. A slight overlapping can be noticed in Figure 19, where is presented PCA statistical analysis of inflammation and metastasis.

5.5 Unknown sample spectra identification and model validation

In the final step, we validated accuracy of our model in identification of unknown sample spectra. For that purpose, a new model was made using only three pathological tissue groups which pose differential diagnostic problems. Normal pleura were excluded from the model. We did not include normal pleura in PCA model, because there are no diagnostic problems in differentiating it. Also, as seen in Figure 14, there is a significant difference in PCA analysis of all spectra between normal pleura and three other groups. Excluding normal pleura from PCA model does not affect validation and results.

New model was built with 150 randomly chosen spectra from each tissue group. The rest of spectra, 60 from each group, were used for model validation. In Figure 21, which also presents principal components in PC1-PC2 space, the new model validated by 180 spectra recorded from mesothelioma, metastatic adenocarcinoma in pleura and inflammations of pleura is shown. Spectra used to create the PCA model are grouped in three separated regions (see Figure 21), with one region for each tissue type.

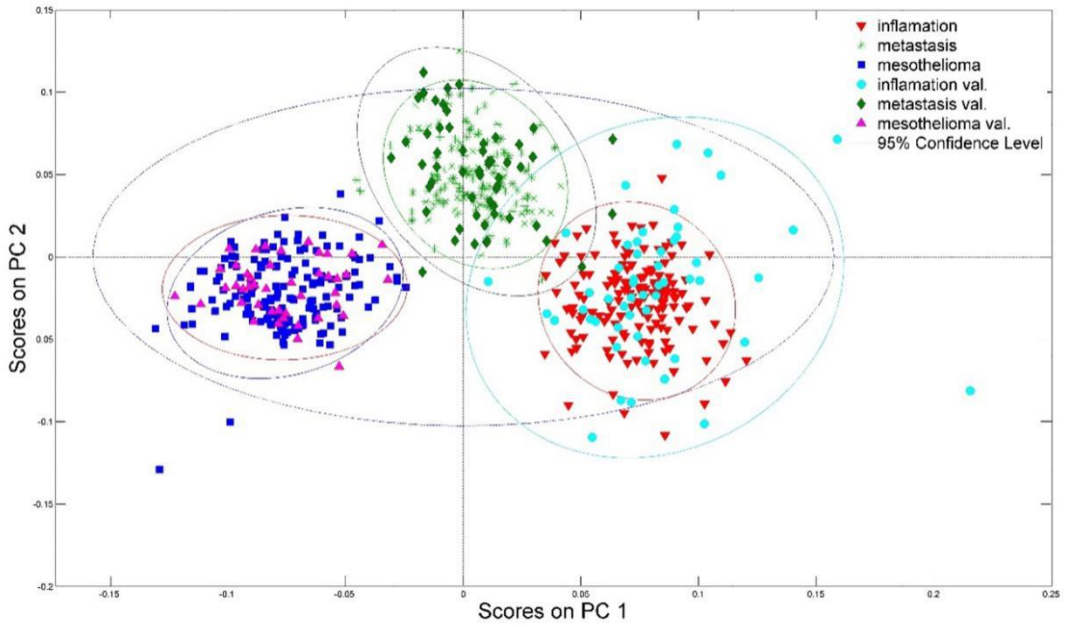

Figure 21. Model random of three groups of samples with pleural lesions.

Every region is encircled by an ellipse surrounding the region where 95% of spectra of the same tissue type are placed. Inside those regions, symbols representing spectra used for modelling are found: blue squares for mesothelioma samples, red triangles for inflammation samples and green stars for metastasis samples. Validation spectra, also visible on Figure 21, are shown with purple triangles for mesotheliomas, turquoise dots for inflammation and green rhombuses representing metastasis. Validation (identified) groups of samples are also surrounded by an ellipse with specific colour representing the region of particular sample type with colour matching the colour of the sample symbols. As can be seen, samples of the same pathology are grouped together and their groups are overlapping with region of the graph where modelling spectra are placed, showing that validation spectra were correctly identified. Although the region of the inflammation identifiers is wider than the others, only small number of spectra is overlapping with the region of metastatic tumours (only two from 210 spectra from metastasis). Furthermore, more than 90% of the spectra from inflammation group are placed in the inflammation region of the graph. Sample heterogeneity or different type of sample inflammation might be the possible reason for wider spread of inflammation spectra in the PC1-PC2 space.

This model was built from randomly chosen spectra and the result was more than 95% certainty in model validation. This model allows us to add more new recorded spectra of pleural lesions and those spectra will be identified by the model as being either mesothelioma, metastasis or inflammatory (reactive) changes.

Table 4. Number of sections for each group of samples used for validation and PCA model.

Tissue type	Sections for validation / patient	Total sections for PCA model	Sections for PCA model / patient	Total sections for validation
Inflammation	15	150	6	60
Mesothelioma	15	150	6	60
Adenocarcinoma	15	150	6	60
Total		450		180

5.6 Loadings

Comparing loadings (Figure 22) and STT results seen in Figure 8, 9, 10, 11, 12 and 13, we can see that the main contribution to differences between spectra are specific wavenumbers used in modelling. A large group of wavenumbers are indicated important (Figure 22) but we can extract the important ones by comparing them to STT results (Figure 8, 9, 10, 11, 12 and 13). These noticed differences are presented with thick lines in difference spectra of the STT plots. Intensive peaks in loadings graph indicate wave numbers that significantly contribute to certain principal components. PC1 loadings are presented on Figure 22. Presented loadings plot (Figure 22) and band assignments from Table 3 suggest that differences in FTIR spectra are connected with DNA, nucleic acids, proteins and lipids vibrational bands. Finding out the reason why these changes are present and what they mean is the aim of future research.

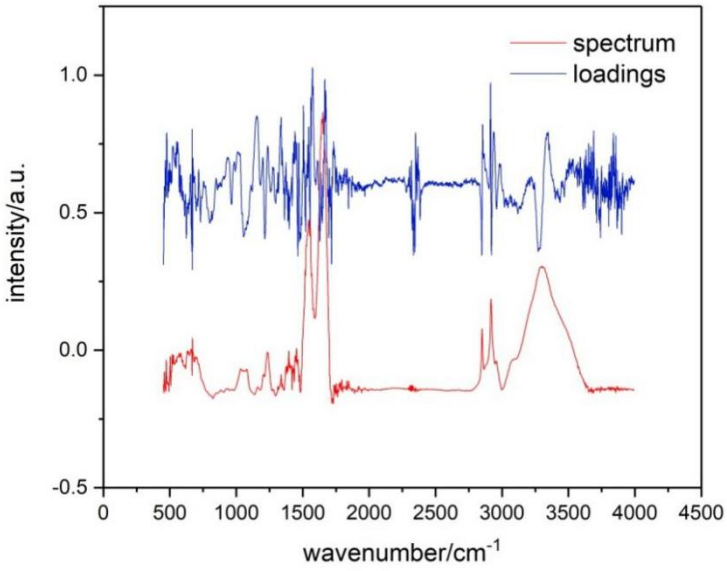

Figure 22. Loadings

6. DISCUSSION

Discriminating between different types of pleural lesions still remains a diagnostic challenge because of their often non-specific or overlapping histopathological appearance (2,5–7). There have been many temptations reflected in a big number of studies for finding a proper panel of immunohistochemical antibodies for differentiating lung adenocarcinoma from mesothelioma, but there is still space for working on it. Also, despite significant progress in that field so far there is no specific stain that can ensure the definitive differential diagnosis between reactive and malignant changes (77). PCA statistical model presented in this research is a promising objective approach for their potential differentiation. As shown above, on the model and its validation, it is visible that spectra from which model was made are clearly separated into three groups, where most of them fall into smaller ellipse which surrounds 95% of the same type of tissue. Validation spectra were also grouped almost in the same area except the fact that there is a slight overlap between inflammation and metastasis validation group. However, their overall separation is still very clear. Furthermore, there is no overlapping of validation spectra between mesothelioma and metastasis group, and between mesothelioma and inflammation group. Based on the results, it is estimated that PCA model accurately identified more than 95% of all validation spectra. For the current model the whole FTIR spectra was used, while, as seen from loadings and STT, not all parts of spectra equally contribute to spectral differences. We assume that some future model can be improved by using only relevant parts of the spectra. Also, certain scattering of the spectra on PCA score graph can be ascribed to small differences in sample preparation and recording conditions. That can be reduced if the details of FTIR recording procedure are standardized. However, the presented model is already very successful in recognizing changes in pleural tissue providing a better approach for tackling challenges in differential diagnostics.

As mentioned earlier, 10 blocks per tissue type were used in our experiment and each block was cut in 21 tissue sections. Consequently, more than 200 sections were produced for each tissue type. Our study altogeteher analysed 670 spectra form 670 tissue sections. For modelling with the principal component analysis, each tissue section can be considered as a separate sample because of the small molecular inhomogeneity's within each tissue block. As can be seen from validation process, the model built with this assumption is successful. Moreover, if the differences between blocks of the same tissue were significant, additional groups of spectra within a single tissue group would appear in PCA and model random results. Because there are no additional groups, we can assume that each section behaves as a

distinct sample of the same tissue type. We showed that this kind of approach to tissue type and pathological changes identification is possible. For clinical application a model with tissue spectra from more patients must be built, so our next step will be to test this model on a larger patient cohort.

With the use of FTIR spectroscopy, we have recorded spectra from the samples already diagnosed with histopathology. FTIR spectroscopy was used to observe parameters like: intensity, band width and position of vibrational band. Peaks in our curves from recorded spectra that correspond to the vibrations of molecules in the cells of observed tissue are shown to be different according to statistical analysis. Using statistical methods, we have connected those changes with tissue type which has resulted in differential diagnosis. From these results, we can conclude that FTIR separates pleural lesions with a high degree of confidence and is an important advancement in diagnosis of pleural pathology.

During the recording process of normal pleura, we have been facing a problem in getting the spectra because of their low cellularity and the presence of lung tissue near it. Then we have peeled fresh lungs from autopsy cases and took pure pleura in blocks. This procedure was quite time-consuming. After recording two pleuras, we decided to quit getting other pleuras because the spectra of normal pleura in PCA statistical analysis were presented very different from the others, making a group in one corner in the PCA chart. It was very obvious that pleura are different from other samples.

In our final model shown above, we excluded spectra recorded on healthy pleura samples. There were several reasons for that decision. First, normal pleura are very thin and the amount of tissue collected during the diagnostic procedure is rather small thereby making it hard to produce samples with recordable infrared absorption. Healthy pleura tissue can also be easily distinguished from pathological tissues by conventional methods so a special model for that purpose is not needed. Second, the model can be successfully built without pleura because the distribution of pathological tissue spectra does not depend on spectra of normal pleura. Comparing the distribution of the spectra in the model where only pathologically changed tissue was used and the one where healthy pleura was included, it is obvious that relative positions of pathological spectra groups and their distributions are similar, in contrast to normal pleura, suggesting that our omission of the healthy pleura group is a correct simplification. Furthermore, PCA statistical analysis of all recorded spectra also shows a visible difference between three pathological and one normal tissue type. It is clearly visible that spectra from healthy pleura formed a separated group, which shows the indubitable spectroscopic difference from the other tissue types.

At the end, another advantage of this procedure must be emphasized. Preparation of samples for histopathology examination, microscopy and the need for IHC analysis is time-consuming and rather expensive. By contrast, in FTIR analysis tissue sections are analysed, therefore time for the preparation of the paraffin block and the cuts remains, but there is no need for immunohistochemistry, and perhaps HE. After the model is built, time necessary for identification of unknown samples is very short, approximately 30 minutes for the complete procedure, so FTIR and PCA modelling promises to be time-saving in comparison to histology. Having in mind how expensive immunohistochemistry is (taking into account the staining machine, microscope and chemicals including antibodies), while for FTIR spectroscopy we need the spectrometer and power, it turns out that it could be also cost-effective in comparison to standard procedure.

Small biopsy samples taken during thoracoscopy usually do not have all the elements for diagnosis of malignancy, like invasion. Immunohistochemistry is essential in confirming the origin of the tumour, having in mind subtypes and similarities between the tumour cells. From laboratory to another, there are similarities at the same time there are differences in proposed panels for differential diagnosis of mesothelioma from lung adenocarcinoma. But, no specific marker was found to give the diagnosis alone. And having in mind different cases reported to be exceptions we can say that in individual cases it is hard enough to give a 100% accurate diagnosis.

To date, there are no standard protocols for using FTIR in everyday work diagnostics, also it is still not commercially available, but the number of research using this method is growing, that tend to reach this goal. In many studies in cancer diagnostics, there are used different samples from liquids like blood, urine and other cell samples, to solid samples too.

As can be seen from the results mentioned in research background, FTIR spectroscopy has found application in different research areas, where essential point is biochemical change of sample compounds. Furthermore, it has been made a progress in optimizing the procedures for sample preparation for spectroscopy.

In a research (Schultz, 2002), FTIR spectroscopy was used to analyse lymphocytes from normal people and patients with chronic lymphocytic leukaemia (CLL), showing the ability to differentiate two types of cells. FTIR spectral changes presented by statistical analysis detected alterations used also for CLL staging and predicting the outcome of drug-treatment in short time (46). The same paper presented that FTIR gathered with statistical analysis of spectra results provide information to differentiate normal, adenoma and carcinoma tissue samples from the thyroid, which presents a diagnostic challenge in

pathology. According to this research, infrared spectroscopy can detect cell alterations which can be used to differentiate cell types that way help pathologists in diagnosis of similar tissue conditions. A research that used frozen section tissues has shown that changes of the biochemical components of normal, hyperplasia, fibroadenoma, ductal carcinoma and invasive ductal carcinoma of the breast can be detected by FTIR and differentiate them in particular pathology group. Endoscopic biopsies using small amount of tissue present a quite challenging samples for diagnostics, but a research using FTIR spectroscopy analysis of gastric samples has shown that this method is very sensitive to cell changes even is small amounts of sample. The research presented that spectral differences of endoscopic gastric samples could differentiate normal, chronic superficial gastritis, atrophic gastritis and cancerous gastric changes (49). Results from different studies are promising that FTIR in near future can be a diagnostic and screening tool in routine clinic work. Sensitivity, specificity and accuracy in diagnostics presented in different studies, make FTIR spectroscopy a desirable method in guiding histopathologists to exclude subjective mistakes and in this way help clinicians to avoid mistreatment of patients. Moreover, advantages of FTIR spectroscopy as a rapid test make it a much needed technique in intraoperative diagnostics, bone and other tumour diagnosis. The results from our study also support the idea of using FTIR spectroscopy as a helpful objective tool in diagnostics of challenging pleural changes.

Having in mind the disadvantages of decalcification process for histological evaluation, FTIR may present novel rapid diagnostic tool in diagnosis of bone tumours, too (68).

The motivation behind this study was to create an objective method to distinguish between three most common types of pathological pleura tissues with accuracy at least comparable to standard pathological methods. Results showed that spectroscopic differences between pleura pathological tissues can be observed and used for PCA model for their recognition. First, we recorded FTIR spectra of different pathology tissues, than we used STT and PCA to show that differences between their spectra exist and then we built the PCA model. Validation of the model showed that accuracy of the model is higher than 95%.

If vibrational spectroscopy in the near future becomes a diagnostic tool, the correlation between its results and histologic evaluations are indisputable, because if both confirm cancer for patient treatment is needed more information like tumour grade, metastasis, therapeutic effects, etc. (1).

Changes in different lesions of pleura proved in our results of Student's T-Test could be a solid ground for further biochemical research. Every band assignment that presents a

difference in particular group could give information on changed molecules of tumour or non-tumour cells, and also could be a question for their belonging place. Answers to issues like the above mentioned, would give us more information for finding new target biochemical and immunohistochemical markers for tumour diagnosis.

As technology is everyday advancing, if our research would be repeated, it could be used spectroscopes equipped with the microscope and evaluate the most representative areas of disease. In that way our results would be proven again and even without possible unwanted effects of surrounding tissue in recording process of spectra.

7. CONCLUSION

Our results show that the model was successful because more than 95% of validation spectra were placed to the group of relevant pathology. From our findings, we can conclude that FTIR spectroscopy combined with PCA is very sensitive and can clearly distinguish different changes in samples with pleural lesions and potentially other types of cancer, in clinical diagnostics and research laboratories. Furthermore, our results suggest that the model can identify the spectra obtained from different pleural lesions. To build clinically usable model with fresh tissue samples further research is needed.

On the other side, to build reliable clinical model additional spectra of tissue samples should be recorded with more precise recording protocols. We also noticed that certain parts of spectra have stronger contribution to spectra separation in PCA model. That fact can be used in order to detect which molecules undergo biochemical changes caused by disease.

This work indicates that FTIR spectroscopy combined with PCA can represent a valuable tool in analysing the still challenging problem of mesothelioma diagnosis.

FTIR spectroscopy overcomes the diagnostic limitations in providing a definitive differential diagnosis between reactive and neoplastic mesothelial cells. Our study can be the foundation for further studies that can focus on the specific molecules that undergo biochemical changes caused by certain disease.

To our knowledge, this is the first study that evaluated the possibilities of using FTIR spectroscopy for differential diagnosis of pleural lesions.

In the future research we can create the model with fresh tissue samples too (from biopsies and/or FNA cytology), for helping everyday diagnostics.

Possible disadvantage of this method is that recording conditions can affect the results, but in order to determine the level of importance, more research and standardized conditions are needed.

8. SAŽETAK

Histopatologija ne može uvijek lako postaviti točnu dijagnozu različitih pleuralnih lezija. Iako je postignut veliki napredak na ovom polju, problem pri razlikovanju između reaktivnih i malignih pleularnih lezija još uvijek potiče na istraživanja za dodatnim dijagnostičkim metodama. Ovo istraživanje, koristeći vibracijsku spektroskopiju i PCA statistički model, predstavlja potencijalno koristan alat za pristup ovom problemu. Objektivna metoda koju ovo istraživanje proučava, temelji se na usporedbi između različitih vrsta pleuralnih lezija i njihovih vibracijskih spektara.

Dobiveni tkivni spektri snimani su infracrvenom spektroskopijom koja omogućava kategoriziranje spektra u različite grupe koristeći stvoren PCA model. Model je stvoren koristeći tkiva poznate patologije kao grupe modela. Validacijski uzorci su korišteni za potvrđivanje funkcionalnosti našeg PCA statističkog modela. T- test je također korišten za usporedbu uzoraka u sparenim grupama.

PCA statistički model je omogućio da se jasno razlikuju spektri između mezotelioma, metastaza i reaktivnih promjena i svrsta ih se u različite grupe.

FTIR spektroskopija u kombinaciji s PCA modelom može razlikovati pleuralne lezije s visokom senzitivnošću i specifičnošću. Ovaj novi pristup može doprinjeti u objektivnom razlikovanju različitih pleuralnih lezija i tako pomoći patologu pri dijagnostičkim dvojbama kod postavljanja dijagnoza na pleuralnih uzorcima ali također baca dodatno svjetlo na biologiju mezotelioma.

9. ABSTRACT

Comparison of pleural lesions using vibrational spectroscopy, 2019; Fatlinda Sadiku Zehri

Histopathology does not always easily provide a correct diagnosis for different pleural lesions. Although great progress was made in this field, the issue of differentiating between reactive and malignant pleural lesions still stimulates the search for additional diagnostic tools. This research, using vibrational spectroscopy and PCA statistical modeling, represents a potentially useful tool to approach the problem. The objective method this research explores is based on the correlation between different types of pleural lesions and their vibrational spectra.

Obtained tissue spectra recorded by infrared spectroscopy allowed categorizing spectra in different groups using a created PCA model. The model was built using tissues of known pathology as the model group. The validation samples were used to confirm the functionality of our PCA statistical model. Students T- test was also used for comparing samples in paired groups.

The PCA statistical model was able to clearly differentiate the spectra of mesothelioma, metastasis and reactive changes, and place them in discrete groups.

FTIR spectroscopy combined with PCA model can differentiate pleural lesions with high sensitivity and specificity. This new approach could contribute in objectively differentiating specific pleural lesions, thus helping pathologists to diagnose difficult pleural samples but also shed additional light into the biology of mesothelioma.

Keywords: Pleura, mesothelioma, reactive changes, metastatic adenocarcinoma, FTIR spectroscopy

10. REFERENCE

1. Dukor R. Vibrational Spectroscopy in the Detection of Cancer. In: Handbook of Vibrational Spectroscopy. 2006.
2. Kadota K, Suzuki K, Sima CS, Rusch VW, Adusumilli PS, Travis WD. Pleomorphic epithelioid diffuse malignant pleural mesothelioma: a clinicopathological review and conceptual proposal to reclassify as biphasic or sarcomatoid mesothelioma. J Thorac Oncol Off Publ Int Assoc Study Lung Cancer. 2011 May;6(5):896–904.
3. Dogan M, Utkan G, Hocazade C, Uncu D, Toptas S, Ozdemir N, et al. The clinicopathological characteristics with long-term outcomes in malignant mesothelioma. Med Oncol. 2014 Oct;31(10):232.
4. Robinson BWS, Lake RA. Advances in malignant mesothelioma. N Engl J Med. 2005 Oct 13;353(15):1591–603.
5. Butnor KJ. My approach to the diagnosis of mesothelial lesions. J Clin Pathol. 2006 Jun;59(6):564–74.
6. Allen TC. Recognition of histopathologic patterns of diffuse malignant mesothelioma in differential diagnosis of pleural biopsies. Arch Pathol Lab Med. 2005 Nov;129(11):1415–20.
7. Sahn SA. Pleural diseases related to metastatic malignancies. Eur Respir J. 1997 Aug;10(8):1907–13.
8. Saleh HA, El-Fakharany M, Makki H, Kadhim A, Masood S. Differentiating reactive mesothelial cells from metastatic adenocarcinoma in serous effusions: the utility of immunocytochemical panel in the differential diagnosis. Diagn Cytopathol. 2009 May;37(5):324–32.
9. Cagle PT, Churg A. Differential diagnosis of benign and malignant mesothelial proliferations on pleural biopsies. Arch Pathol Lab Med. 2005 Nov;129(11):1421–7.
10. Travis WD, Brambilla E, Burke AP, Marx A, Nicholson AG. WHO classification of Tumors of the Lung, Pleura, Thymus and Heart. 4th edition Lyon:IARC;2015.
11. Weidner N, R. Cote, Suster S, Weiss L. Modern Surgical Pathology. 2nd edition Philadelphia:Saunders;2009.
12. Pinheiro C, Longatto-Filho A, Soares TR, Pereira H, Bedrossian C, Michael C, et al. CD147 immunohistochemistry discriminates between reactive mesothelial cells and malignant mesothelioma. Diagn Cytopathol. 2012 Jun;40(6):478–83.

13. Kitazume H, Kitamura K, Mukai K, Inayama Y, Kawano N, Nakamura N, et al. Cytologic differential diagnosis among reactive mesothelial cells, malignant mesothelioma, and adenocarcinoma: utility of combined E-cadherin and calretinin immunostaining. Cancer. 2000 Feb 25;90(1):55–60.

14. Politi E, Kandaraki C, Apostolopoulou C, Kyritsi T, Koutselini H. Immunocytochemical panel for distinguishing between carcinoma and reactive mesothelial cells in body cavity fluids. Diagn Cytopathol. 2005 Mar;32(3):151–5.

15. Comin CE, Novelli L, Boddi V, Paglierani M, Dini S. Calretinin, thrombomodulin, CEA, and CD15: a useful combination of immunohistochemical markers for differentiating pleural epithelial mesothelioma from peripheral pulmonary adenocarcinoma. Hum Pathol. 2001 May;32(5):529–36.

16. Marchevsky AM. Application of immunohistochemistry to the diagnosis of malignant mesothelioma. Arch Pathol Lab Med. 2008 Mar;132(3):397–401.

17. Ordóñez NG. The diagnostic utility of immunohistochemistry in distinguishing between epithelioid mesotheliomas and squamous carcinomas of the lung: a comparative study. Mod Pathol Off J U S Can Acad Pathol Inc. 2006 Mar;19(3):417–28.

18. King JE, Thatcher N, Pickering CA, Hasleton PS. Sensitivity and specificity of immunohistochemical markers used in the diagnosis of epithelioid mesothelioma: a detailed systematic analysis using published data. Histopathology. 2006 Feb;48(3):223–32.

19. Sandeck HP, Røe OD, Kjærheim K, Willén H, Larsson E. Re-evaluation of histological diagnoses of malignant mesothelioma by immunohistochemistry. Diagn Pathol. 2010 Jul 6;5:47.

20. Abutaily AS, Addis BJ, Roche WR. Immunohistochemistry in the distinction between malignant mesothelioma and pulmonary adenocarcinoma: a critical evaluation of new antibodies. J Clin Pathol. 2002 Sep;55(9):662–8.

21. Andrici J, Sheen A, Sioson L, Wardell K, Clarkson A, Watson N, et al. Loss of expression of BAP1 is a useful adjunct, which strongly supports the diagnosis of mesothelioma in effusion cytology. Mod Pathol. 2015 Oct;28(10):1360–8.

22. Sheffield BS, Hwang HC, Lee AF, Thompson K, Rodriguez S, Tse CH, et al. BAP1 immunohistochemistry and p16 FISH to separate benign from malignant mesothelial proliferations. Am J Surg Pathol. 2015 Jul;39(7):977–82.

23. Cigognetti M, Lonardi S, Fisogni S, Balzarini P, Pellegrini V, Tironi A, et al. BAP1 (BRCA1-associated protein 1) is a highly specific marker for differentiating mesothelioma from reactive mesothelial proliferations. Mod Pathol. 2015 Aug;28(8):1043–57.

24. Hida T, Hamasaki M, Matsumoto S, Sato A, Tsujimura T, Kawahara K, et al. BAP1 immunohistochemistry and p16 FISH results in combination provide higher confidence in malignant pleural mesothelioma diagnosis: ROC analysis of the two tests. Pathol Int. 2016 Oct;66(10):563–70.

25. Monaco S, Mehrad M, Dacic S. Recent Advances in the Diagnosis of Malignant Mesothelioma: Focus on Approach in Challenging Cases and in Limited Tissue and Cytologic Samples. Adv Anat Pathol. 2018 Jan;25(1):24–30.

26. Matsubara T, Toyokawa G, Yamada Y, Nabeshima K, Haratake N, Kozuma Y, et al. A Case of the Resected Lymphohistiocytoid Mesothelioma: BAP1 Is a Key of Accurate Diagnosis. Anticancer Res. 2017;37(12):6937–41.

27. Hida T, Hamasaki M, Matsumoto S, Sato A, Tsujimura T, Kawahara K, et al. Immunohistochemical detection of MTAP and BAP1 protein loss for mesothelioma diagnosis: Comparison with 9p21 FISH and BAP1 immunohistochemistry. Lung Cancer. 2017;104:98–105.

28. Berg KB, Dacic S, Miller C, Cheung S, Churg A. Utility of Methylthioadenosine Phosphorylase Compared With BAP1 Immunohistochemistry, and CDKN2A and NF2 Fluorescence In Situ Hybridization in Separating Reactive Mesothelial Proliferations From Epithelioid Malignant Mesotheliomas. Arch Pathol Lab Med. 2018 Jul 30; 142(12):1549-53.

29. Monaco S, Mehrad M, Dacic S. Recent Advances in the Diagnosis of Malignant Mesothelioma: Focus on Approach in Challenging Cases and in Limited Tissue and Cytologic Samples. Adv Anat Pathol. 2018 Jan;25(1):24–30.

30. Churg A, Hwang H, Tan L, Qing G, Taher A, Tong A, et al. Malignant mesothelioma in situ. Histopathology. 2018 May;72(6):1033–8.

31. Tochigi N, Attanoos R, Chirieac LR, Allen TC, Cagle PT, Dacic S. p16 Deletion in sarcomatoid tumors of the lung and pleura. Arch Pathol Lab Med. 2013 May;137(5):632–6.

32. Marchevsky AM, LeStang N, Hiroshima K, Pelosi G, Attanoos R, Churg A, et al. The differential diagnosis between pleural sarcomatoid mesothelioma and spindle cell/pleomorphic (sarcomatoid) carcinomas of the lung: evidence-based guidelines from the International Mesothelioma Panel and the MESOPATH National Reference Center. Hum Pathol. 2017;67:160–8.

33. Monaco SE, Shuai Y, Bansal M, Krasinskas AM, Dacic S. The diagnostic utility of p16 FISH and GLUT-1 immunohistochemical analysis in mesothelial proliferations. Am J Clin Pathol. 2011 Apr;135(4):619–27.

34. Chiosea S, Krasinskas A, Cagle PT, Mitchell KA, Zander DS, Dacic S. Diagnostic importance of 9p21 homozygous deletion in malignant mesotheliomas. Mod Pathol. 2008 Jun;21(6):742–7.

35. Schürch CM, Forster S, Brühl F, Yang SH, Felley-Bosco E, Hewer E. The “don’t eat me” signal CD47 is a novel diagnostic biomarker and potential therapeutic target for diffuse malignant mesothelioma. Oncoimmunology. 2017;7(1):e1373235.

36. Kawai T, Watanabe M, Takagi K. Thoracoscopic anatomy, significance of pathologic findings in thoracoscopic open lung biopsy, and pleural mesothelioma. Nihon Kyobu Shikkan Gakkai Zasshi. 1994 Dec;32 Suppl:142–7.

37. Gasper R, Mijatovic T, Bénard A, Derenne A, Kiss R, Goormaghtigh E. FTIR spectral signature of the effect of cardiotonic steroids with antitumoral properties on a prostate cancer cell line. Biochim Biophys Acta. 2010 Nov;1802(11):1087–94.

38. Gasper R, Vandenbussche G, Goormaghtigh E. Ouabain-induced modifications of prostate cancer cell lipidome investigated with mass spectrometry and FTIR spectroscopy. Biochim Biophys Acta. 2011 Mar;1808(3):597–605.

39. Sule-Suso J, Forsyth NR, Untereiner V, Sockalingum GD. Vibrational spectroscopy in stem cell characterisation: is there a niche? Trends biothechnol. 2014;32(5):254-262.

40. Movasaghi Z, Rehman S, Rehman I. Fourier Transform Infrared (FTIR) Spectroscopy of Biological Tissues. App Spectrosc Rev. 2008;43:2.

41. Dimitrova M, Ivanova D, Karamancheva I, Milev A, Dobrev I. Application of FTIR-spectroscopy for diagnosis of breast cancer tumors. J Univ Chem Technol Metall. 2009 Jan 1;44(3):297-300.

42. Rak S, De Zan T, Stefulj J, Kosović M, Gamulin O, Osmak M. FTIR spectroscopy reveals lipid droplets in drug resistant laryngeal carcinoma cells through detection of increased ester vibrational bands intensity. Analyst. 2014 Jul 7;139(13):3407–15.

43. Sheng D, Xu F, Yu Q, Fang T, Xia J, Li S, Wang X. A study of structural differences between liver cancer cells and normal liver cells using FTIR spectroscopy. J Mol Struct. 2015;1099:18-23.

44. Mazur AI, Monahan JL, Miljković M, Laver N, Diem M, Bird B. Vibrational spectroscopic changes of B-lymphocytes upon activation. J Biophotonics. 2013 Jan;6(1):101–9.

45. Mitchell AL, Gajjar KB, Theophilou G, Martin FL, Martin-Hirsch PL. Vibrational spectroscopy of biofluids for disease screening or diagnosis: translation from the laboratory to a clinical setting. J Biophotonics. 2014 Apr;7(3–4):153–65.

46. Schultz CP. The potential role of Fourier transform infrared spectroscopy and imaging in cancer diagnosis incorporating complex mathematical methods. Technol Cancer Res Treat. 2002 Apr;1(2):95–104.

47. Wang HP, Wang HC, Huang YJ. Microscopic FTIR studies of lung cancer cells in pleural fluid. Sci Total Environ. 1997 Oct 1;204(3):283–7.

48. Sahu RK, Mordechai S. Fourier transform infrared spectroscopy in cancer detection. Future Oncol. 2005 Oct;1(5):635–47.

49. Li Q-B, Sun X-J, Xu Y-Z, Yang L-M, Zhang Y-F, Weng S-F, et al. Diagnosis of gastric inflammation and malignancy in endoscopic biopsies based on Fourier transform infrared spectroscopy. Clin Chem. 2005 Feb;51(2):346–50.

50. Lewis PD, Lewis KE, Ghosal R, Bayliss S, Lloyd AJ, Wills J, et al. Evaluation of FTIR spectroscopy as a diagnostic tool for lung cancer using sputum. BMC Cancer. 2010 Nov 23;10:640.

51. Wu M, Zhang W, Tian P, Ling X, Xu ZB. Intraoperative diagnosis of thyroid diseases by fourier transform infrared spectroscopy based on support vector machine. Int J Clin Exp Med. 2016;9(2):2351-2358.

52. Liu H, Su Q, Sheng D, Zheng W, Wang X. Comparison of red blood cells from gastric cancer patients and healthy persons using FTIR spectroscopy. J Mol Struct. 2017 Feb 15;1130:33-37.

53. Ollesch J, Theegarten D, Altmayer M, Darwiche K, Hager T, Stamatis G, et al. An infrared spectroscopic blood test for non-small cell lung carcinoma and subtyping into pulmonary squamous cell carcinoma or adenocarcinoma. Biomed Spectrosc Imaging. 2016 Jan 1;5(2):129–44.

54. Tian P, Zhang W, Zhao H, Lei Y, Cui L, Zhang Y, et al. Intraoperative detection of sentinel lymph node metastases in breast carcinoma by Fourier transform infrared spectroscopy. Br J Surg. 2015 Oct;102(11):1372–9.

55. Bunaciu AA, Hoang VD, Aboul-Enein HY. Applications of FT-IR spectrophotometry in cancer diagnostics. Crit Rev Anal Chem. 2015;45(2):156–65.

56. Andrus PG, Strickland RD. Cancer grading by Fourier transform infrared spectroscopy. Biospectrosc. 1998;4(1):37–46.

57. Kaznowska E, Depciuch J, Szmuc K, Cebulski J. Use of FTIR spectroscopy and PCA-LDC analysis to identify cancerous lesions within the human colon. J Pharm Biomed Anal. 2017 Feb 5;134:259–68.

58. Devi G, Devi R, Gunasekaran S. FTIR spectroscopic study on benign and cancerous human breast tissues - a run chart analysis. Int J Pharmaceut. 2010;2:2.

59. Hughes C, Iqbal-Wahid J, Brown M, Shanks JH, Eustace A, Denley H, et al. FTIR microspectroscopy of selected rare diverse sub-variants of carcinoma of the urinary bladder. J Biophotonics. 2013 Jan;6(1):73–87.

60. Siqueira L, Lima K. A decade (2004 - 2014) of FTIR prostate cancer spectroscopy studies: An overview of recent advancements. TrAC Trends Anal Chem. 2016 Sep;82:208-221.

61. Baker MJ, Gazi E, Brown MD, Shanks JH, Gardner P, Clarke NW. FTIR-based spectroscopic analysis in the identification of clinically aggressive prostate cancer. Br J Cancer. 2008 Dec;99(11):1859–66.

62. Shirazi FH, Wong PTT, Goe R. Interaction of Cisplatin with Cellular Macromolecules: A Fourier Transform Infrared Spectroscopy Study. Iran J Pharm Res. 2003 Nov; 2(1):11–5.

63. Neves ACO, Silva PP, Morais CLM, Miranda CG, Crispim JCO, Lima KMG. ATR-FTIR and multivariate analysis as a screening tool for cervical cancer in women from northeast Brazil: a biospectroscopic approach. RSC Adv. 2016 Oct 14;6(102):99648–55.

64. Frost J, Ludeman L, Hillaby K, Gornall R, Lloyd G, Kendall C, et al. Identification of cancer associated molecular changes in histologically benign vulval disease found in association with vulval squamous cell carcinoma using Fourier transform infrared spectroscopy. Anal Methods. 2016 Nov 14;8(48):8452–60.

65. Barcot O, Balarin M, Gamulin O, Jezek D, Romac P, Brnjas-Kraljević J. Investigation of spermatozoa and seminal plasma by fourier transform infrared spectroscopy. Appl Spectrosc. 2007 Mar;61(3):309–13.

66. Gamulin O, Serec K, Bilić V, Balarin M, Kosović M, Drmić D, et al. Monitoring the healing process of rat bones using Raman spectroscopy. J Mol Struct. 2013 Jul 24;1044:308–13.

67. Huang H, Feng S, Chen W, Yu Y, Lin D, Chen R. Study on Fracture Healing with Small-Splint-Fixation Therapy by Near-Infrared Raman Spectroscopy. J Spectrosc. 2013:ID 810247, http://dx.doi.org/10.1155/2013/810247

68. Anastassopoulou J, Kyriakidou M, Kyriazis S, Kormas TH, Mavrogenis AF, Dritsa V, et al. An FT-IR Spectroscopic Study of Metastatic Cancerous Bones. In: Infrared Spectroscopy - Anharmonicity of Biomolecules, Crosslinking of Biopolymers, Food Quality and Medical Application; 2015. http://dx.doi.org/10.5772/58910

69. Lima KMG, Gajjar KB, Martin-Hirsch PL, Martin FL. Segregation of ovarian cancer stage exploiting spectral biomarkers derived from blood plasma or serum analysis: ATR-FTIR spectroscopy coupled with variable selection methods. Biotechnol Prog. 2015 Jun;31(3):832–9.

70. Theophilou G, G. Lima KM, L. Martin-Hirsch P, F. Stringfellow H, L. Martin F. ATR-FTIR spectroscopy coupled with chemometric analysis discriminates normal, borderline and malignant ovarian tissue: classifying subtypes of human cancer. Analyst. 2016;141(2):585–94.

71. Koss LG, Melamed RG. Koss` Diagnostic Cytology and its Histopathologic bases. 5th edition Philadelphia: Lippinkott Wiliam & Wilkins;2006.

72. Mescher AL. Junqueira's Basic Histology: Text And Atlas. 12th edition New York:McGraw-Hill;2010.

73. Rahman N, Clelland CA, Lee YCG. The pleural cavity. In: encyclopedia of respiratory diseases. Oxford:Elsevier;2006. p. 397-402.

74. Rosai J. Rosai and Ackerman`s Surgical Pathology. 10th edition:Elsevier Inc;2012.

75. Lai-Fook SJ. Pleural mechanics and fluid exchange. Physiol Rev. 2004 Apr;84(2):385–410.

76. Jones JSP. The Pleura in Health and Disease. Lung. 2001 Dec 1;179(6):397–413.

77. Husain AN, Colby TV, Ordóñez NG, Allen TC, Attanoos RL, Beasley MB, et al. Guidelines for Pathologic Diagnosis of Malignant Mesothelioma 2017 Update of the Consensus Statement From the International Mesothelioma Interest Group. Arch Pathol Lab Med. 2018 Jan;142(1):89–108.

78. Curin K, Sarić M, Strnad M. Incidence of malignant pleural mesothelioma in coastal and continental Croatia: epidemiological study. Croat Med J. 2002 Aug;43(4):498–502.

79. Dečković-Vukres V, Ćorić T, Tomić B, Erceg M, Mihel S, Ivičević Uhernik A, et al. Pojavnost bolesti uzrokovanih azbestom u Republici Hrvatskoj u razdoblju od 2002. do 2007. Arh Hig Rada Toksikol. 2009 Nov 2;60(Supplement):23–9.

80. The Croatian Institute of Public Health. Cancer Register of the Republic of Croatia (Registar za rak Republike Hrvatske). Incidencija raka u Hrvatskoj 2015. Bilten 40. Zagreb: Hrvatski zavod za javno zdravstvo (Croatian Public Health Institute);2018.

81. Haber SE, Haber JM. Malignant mesothelioma: a clinical study of 238 cases. Ind Health. 2011;49(2):166–72.

82. Geltner C, Errhalt P, Baumgartner B, Ambrosch G, Machan B, Eckmayr J, et al. Management of malignant pleural mesothelioma - part 1: epidemiology, diagnosis, and

staging : Consensus of the Austrian Mesothelioma Interest Group (AMIG). Wien Klin Wochenschr. 2016 Sep;128(17):611–7.

83. Gordon R, Fitzgerald S, Millette J. Asbestos in commercial cosmetic talcum powder as a cause of mesothelioma in women. Int J Occup Environ Health. 2015;21(4):347–8.

84. Selikoff IJ, Churg J, Hammond EC. Relation between Exposure to Asbestos and Mesothelioma. N Engl J Med. 1965;272:560-565.

85. Yang H, Testa JR, Carbone M. Mesothelioma Epidemiology, Carcinogenesis and Pathogenesis. Curr Treat Options Oncol. 2008 Jun;9(2–3):147–57.

86. Hodgson JT, Darnton A. The quantitative risks of mesothelioma and lung cancer in relation to asbestos exposure. Ann Occup Hyg. 2000 Dec;44(8):565–601.

87. Toyokuni S. Mechanisms of asbestos-induced carcinogenesis. Nagoya J Med Sci. 2009 Feb;71(1–2):1–10.

88. Carbone M, Yang H. Targeting Mechanisms of Asbestos and Erionite Carcinogenesis in Mesothelioma. Clin Cancer Res. 2012 Feb 1;18(3):598–604.

89. Lazarus AA, Philip A. Asbestosis. Dis Mon. 2011 Jan;57(1):14–26.

90. Mayo Clinic. Asbestosis - Symptoms and causes [Internet]. Available from: https://www.mayoclinic.org/diseases-conditions/asbestosis/symptoms-causes/syc-20354637

91. Mesothelioma Center - Vital Services for Cancer Patients & Families. Asbestosis Diagnosis: The Diagnostic Process, Symptoms and Scans [Internet]. Available from: https://www.asbestos.com/asbestosis/diagnosis/

92. Steele JPC, Klabatsa A. Chemotherapy options and new advances in malignant pleural mesothelioma. Ann Oncol. 2005 Mar;16(3):345–51.

93. Sage AP, Martinez VD, Minatel BC, Pewarchuk ME, Marshall EA, MacAulay GM, et al. Genomics and Epigenetics of Malignant Mesothelioma. High-Throughput. 2018 Jul 27;7(3).

94. Zauderer MG, Bott M, McMillan R, Sima CS, Rusch V, Krug LM, et al. Clinical characteristics of patients with malignant pleural mesothelioma harboring somatic BAP1 mutations. J Thorac Oncol. 2013 Nov;8(11):1430–3.

95. Cooper SP, Fraire AE, Buffler PA, Greenberg SD, Langston C. Epidemiologic aspects of childhood mesothelioma. Pathol Immunopathol Res. 1989;8(5–6):276–86.

96. Grundy GW, Miller RW. Malignant mesothelioma in childhood. Report of 13 cases. Cancer. 1972 Nov;30(5):1216–8.

97. Kliment CR, Clemens K, Oury TD. North American Erionite-Associated Mesothelioma with Pleural Plaques and Pulmonary Fibrosis: A Case Report. Int J Clin Exp Pathol. 2008 Nov 25;2(4):407–10.

98. Emri S, Demir A, Dogan M, Akay H, Bozkurt B, Carbone M, et al. Lung diseases due to environmental exposures to erionite and asbestos in Turkey. Toxicol Lett. 2002 Feb 28;127(1–3):251–7.

99. Huncharek M. Non-asbestos related diffuse malignant mesothelioma. Tumori. 2002 Feb;88(1):1–9.

100. Cavazza A, Travis LB, Travis WD, Wolfe JT, Foo ML, Gillespie DJ, et al. Post-irradiation malignant mesothelioma. Cancer. 1996 Apr 1;77(7):1379–85.

101. Muscat JE, Huncharek M. Dietary intake and the risk of malignant mesothelioma. Br J Cancer. 1996;73(9):1122-1125.

102. Schiffman MH, Pickle LW, Fontham E, Zahm SH, Falk R, Mele J, et al. Case-control study of diet and mesothelioma in Louisiana. Cancer Res. 1988 May 15;48(10):2911–5.

103. Kent M, Rice D, Flores R. Diagnosis, staging, and surgical treatment of malignant pleural mesothelioma. Curr Treat Options Oncol. 2008 Jun;9(2–3):158–70.

104. Cheah HM, Lansley SM, Varano Della Vergiliana JF, Tan AL, Thomas R, Leong SL, et al. Malignant pleural fluid from mesothelioma has potent biological activities. Respirology. 2017;22(1):192–9.

105. Adams VI, Unni KK, Muhm JR, Jett JR, Ilstrup DM, Bernatz PE. Diffuse malignant mesothelioma of pleura. Diagnosis and survival in 92 cases. Cancer. 1986 Oct 1;58(7):1540–51.

106. Fujimoto N, Gemba K, Asano M, Fuchimoto Y, Wada S, Ono K, et al. Hyaluronic acid in the pleural fluid of patients with malignant pleural mesothelioma. Respir Investig. 2013 Jun;51(2):92–7.

107. Creaney J, Dick IM, Segal A, Musk AW, Robinson BWS. Pleural effusion hyaluronic acid as a prognostic marker in pleural malignant mesothelioma. Lung Cancer. 2013 Dec 1;82(3):491–8.

108. Scherpereel A, Astoul P, Baas P, Berghmans T, Clayson H, de Vuyst P, et al. Guidelines of the European Respiratory Society and the European Society of Thoracic Surgeons for the management of malignant pleural mesothelioma. Eur Respir J. 2010 Mar;35(3):479–95.

109. Roger E, Tuengerthal S, Schoenberg SO. The role of new imaging techniques in diagnosis and staging of malignant pleural mesothelioma. Curr Opin Oncol. 2003;15(2):131-138.

110. Wang ZJ, Reddy GP, Gotway MB, Higgins CB, Jablons DM, Ramaswamy M, et al. Malignant pleural mesothelioma: evaluation with CT, MR imaging, and PET. Radiographics. 2004 Feb;24(1):105–19.

111. Tertemiz KC, Ozgen Alpaydin A, Gurel D, Savas R, Gulcu A, Akkoclu A. Multiple distant metastases in a case of malignant pleural mesothelioma. Respir Med Case Rep. 2014 Aug 8;13:16–8.

112. Sibio S, Sammartino P, Accarpio F, Biacchi D, Cornali T, Cardi M, et al. Metastasis of pleural mesothelioma presenting as bleeding colonic polyp. Ann Thorac Surg. 2011 Nov;92(5):1898–901.

113. Hirooka A, Tamiya A, Kanazu M, Nonaka J, Yonezawa T, Asami K, et al. Brain Metastasis of Pleural Mesothelioma after a Subarachnoid Hemorrhage. Intern Med. 2016;55(7):779–81.

114. Higginson DS, Brahmer J, Tufano RP, Bajaj GK. Pleural mesothelioma metastatic to tongue. J Clin Oncol. 2007 May 20;25(15):2133–5.

115. Cheng W-F, Berkman AW. Malignant mesothelioma with bone metastases. Med Pediatr Oncol. 1990 Jan 1;18(2):165–8.

116. Cassarino DS, Xue W, Shannon KJ. Widespread cutaneous and perioral metastases of mesothelioma. J Cutan Pathol. 2003 Oct 1;30(9):582–5.

117. Panadero RF. Diagnosis and treatment of malignant pleural mesothelioma. Arch Bronconeumol. 2015 Apr;51(4):177–84.

118. Shanks JH, Harris M, Banerjee SS, Eyden BP, Joglekar VM, Nicol A, et al. Mesotheliomas with deciduoid morphology: a morphologic spectrum and a variant not confined to young females. Am J Surg Pathol. 2000 Feb;24(2):285–94.

119. Mašić S, Brčić L, Krušlin B, Šepac A, Pigac B, Stančić-Rokotov D, et al. Expression of plakophilin 3 in diffuse malignant pleural mesothelioma. Histol Histopathol. 2018 Sep;33(9):995–1004.

120. Corson JM. Pathology of mesothelioma. Thorac Surg Clin. 2004 Nov 1;14(4):447–60.

121. Rusch VW, Venkatraman E. The importance of surgical staging in the treatment of malignant pleural mesothelioma. J Thorac Cardiovasc Surg. 1996 Apr;111(4):815–26.

122. Nicholson AG, Tsao MS, Travis WD, Patil DT, Galateau-Salle F, Marino M, et al. Eighth Edition Staging of Thoracic Malignancies: Implications for the Reporting Pathologist. Arch Pathol Lab Med. 2018 May;142(5):645–61.

123. Bonomi M, De Filippis C, Lopci E, Gianoncelli L, Rizzardi G, Cerchiaro E, et al. Clinical staging of malignant pleural mesothelioma: current perspectives. Lung Cancer Targets Ther. 2017 Aug 18;8:127–39.

124. Mesothelioma Center - Vital Services for Cancer Patients & Families. Mesothelioma Staging Systems - TNM, Brigham & Butchart [Internet]. Available from: https://www.asbestos.com/mesothelioma/staging-systems/

125. Kindler HL, Ismaila N, Armato SG, Bueno R, Hesdorffer M, Jahan T, et al. Treatment of Malignant Pleural Mesothelioma: American Society of Clinical Oncology Clinical Practice Guideline. J Clin Oncol. 2018 Jan 18;36(13):1343–73.

126. Kindler HL, Ismaila N, Hassan R. Treatment of Malignant Pleural Mesothelioma: American Society of Clinical Oncology Clinical Practice Guideline Summary. J Oncol Pract. 2018;14(4):256–64.

127. Schunselaar LM, Zwart W, Baas P. Targeting BAP1: a new paradigm for mesothelioma. Lung Cancer. 2017;109:145–6.

128. Kim M-C, Hwang S-H, Kim N-Y, Lee H-S, Ji S, Yang Y, et al. Hypoxia promotes acquisition of aggressive phenotypes in human malignant mesothelioma. BMC Cancer. 2018 Aug 15;18(1):819.

129. Herndon JE, Green MR, Chahinian AP, Corson JM, Suzuki Y, Vogelzang NJ. Factors predictive of Survival Among 337 patients with mesothelioma treated between 1984 and 1994 by the Cancer and Leukemia Group B. Chest. 1998;113(3):723-731.

130. Kadota K, Villena-Vargas J, Nitadori J-I, Sima CS, Jones DR, Travis WD, et al. Tumoral CD10 expression correlates with aggressive histology and prognosis in patients with malignant pleural mesothelioma. Ann Surg Oncol. 2015 Sep;22(9):3136–43.

131. Baumann F, Flores E, Napolitano A, Kanodia S, Taioli E, Pass H, et al. Mesothelioma patients with germline BAP1 mutations have 7-fold improved long-term survival. Carcinogenesis. 2015 Jan;36(1):76–81.

132. McGregor SM, Dunning R, Hyjek E, Vigneswaran W, Husain AN, Krausz T. BAP1 facilitates diagnostic objectivity, classification, and prognostication in malignant pleural mesothelioma. Hum Pathol. 2015 Nov;46(11):1670–8.

133. Agalioti T, Giannou AD, Stathopoulos GT. Pleural involvement in lung cancer. J Thorac Dis. 2015 Jun;7(6):1021–30.

134. Chen S-F, Lin Y-S, Jao S-W, Chang Y-C, Liu C-L, Lin Y-J, et al. Pulmonary Adenocarcinoma in Malignant Pleural Effusion Enriches Cancer Stem Cell Properties during Metastatic Cascade. PloS One. 2013 May 1;8(5):e54659.

135. Roberts F, Harper CM, Downie I, Burnett RA. Immunohistochemical analysis still has a limited role in the diagnosis of malignant mesothelioma. A study of thirteen antibodies. Am J Clin Pathol. 2001 Aug;116(2):253–62.

136. Gattuso P, Reddy VB, David O, Spitz DJ, Haber MH. Differential Diagnosis in Surgical Pathology. 2nd edition Philadelphia:Saunders;2010.

137. Suzuki K, Kusumoto M, Watanabe S, Tsuchiya R, Asamura H. Radiologic clasification of small adenocarcinoma of the lung: Radiologic-Pathologic correlation and its prognostic impact. Ann Thorac Surg. 2006 Feb;81(2):413-9.

138. Popper HH. Progression and metastasis of lung cancer. Cancer Metast Rev. 2016;35:75–91.

139. Lucas DR, Pass HI, Madan SK, Adsay NV, Wali A, Tabaczka P, et al. Sarcomatoid mesothelioma and its histological mimics: a comparative immunohistochemical study. Histopathology. 2003 Mar;42(3):270–9.

140. Soomro IN, Oliveira R, Ronan J, Chaudry ZR, Johnson J. Expression of mesothelial markers in malignant mesotheliomas: an immunohistochemical evaluation of 173 cases. J Pak Med Assoc. 2005 May;55(5):205–9.

141. Trupiano JK, Geisinger KR, Willingham MC, Manders P, Zbieranski N, Case D, et al. Diffuse malignant mesothelioma of the peritoneum and pleura, analysis of markers. Mod Pathol. 2004 Apr;17(4):476–81.

142. Soini Y, Kinnula V, Kahlos K, Pääkkö P. Claudins in differential diagnosis between mesothelioma and metastatic adenocarcinoma of the pleura. J Clin Pathol. 2006 Mar;59(3):250–4.

143. Kushitani K, Takeshima Y, Amatya VJ, Furonaka O, Sakatani A, Inai K. Immunohistochemical marker panels for distinguishing between epithelioid mesothelioma and lung adenocarcinoma. Pathol Int. 2007 Apr;57(4):190–9.

144. Panjković M, Lovrenski A, Eri Z, Usaj SK, Tegeltija D, Krcedinac J. The role of immunohistochemical evaluation in the diagnosis of malignant mesothelioma of the pleura. Vojnosanit Pregl. 2013 Nov;70(11):1010–4.

145. Carella R, Deleonardi G, D'Errico A, Salerno A, Egarter-Vigl E, Seebacher C, et al. Immunohistochemical panels for differentiating epithelial malignant mesothelioma from lung

adenocarcinoma: a study with logistic regression analysis. Am J Surg Pathol. 2001 Jan;25(1):43–50.

146. Ordóñez NG. Immunohistochemical diagnosis of epithelioid mesothelioma: an update. Arch Pathol Lab Med. 2005 Nov;129(11):1407–14.

147. Cury PM, Butcher DN, Corrin B, Nicholson Ag. The use of histological and immunohistochemical markers to distinguish pleural malignant mesothelioma and in situ mesothelioma from reactive mesothelial hyperplasia and reactive pleural fibrosis. J Pathol. 1999;189:251-257.

148. Richter G, Heidersdorf H, Hirschfeld D, Krebbel F. Positive TTF-1 Expression in Malignant Mesothelioma: A Case Report. Am J Case Rep. 2016 Mar 4;17:133–6.

149. Su X-Y, Li G-D, Liu W-P, Xie B, Jiang Y-H. Cytological differential diagnosis among adenocarcinoma, epithelial mesothelioma, and reactive mesothelial cells in serous effusions by immunocytochemistry. Diagn Cytopathol. 2011 Dec;39(12):900–8.

150. Kimura F, Okayasu I, Kakinuma H, Satoh Y, Kuwao S, Saegusa M, et al. Differential Diagnosis of Reactive Mesothelial Cells and Malignant Mesothelioma Cells Using the Cell Proliferation Markers Minichromosome Maintenance Protein 7, Geminin, Topoisomerase II Alpha and Ki-67. Acta Cytol. 2013;57(4):384–90.

151. Hasteh F, Lin GY, Weidner N, Michael CW. The use of immunohistochemistry to distinguish reactive mesothelial cells from malignant mesothelioma in cytologic effusions. Cancer Cytopathol. 2010 Apr 25;118(2):90–6.

152. Ghanim B, Klikovits T, Hoda MA, Lang G, Szirtes I, Setinek U, et al. Ki67 index is an independent prognostic factor in epithelioid but not in non-epithelioid malignant pleural mesothelioma: a multicenter study. Br J Cancer. 2015 Mar;112(5):783–92.

153. Lattermann A, Matthäus C, Bergner N, Beleites C, Romeike BF, Krafft C, et al. Characterization of atherosclerotic plaque depositions by Raman and FTIR imaging. J Biophotonics. 2013 Jan;6(1):110–21.

154. Jackson M, Mantsch HH. Pathology by Infrared and Raman Spectroscopy. Biomed App. 2006. https://doi.org/10.1002/0470027320.s8101

155. Ristić, D. Depozicija i karakterizacija nanokristalnog silicija [dissertation]. Zagreb: University of Zagreb, Faculty of Science;2010

156. Sun DW. Spectroscopy for Food Quality Analysis and Control. Academic Press;2009.

157. Ozek NS, Tuna S, Erson-Bensan E, Severcan F. Characterization of microARN-125b expression in MCF7 breast cancer cells by ATR-FTIR spectroscopy. Analyst. 2010 Dec;135(12):3094-102.

158. Bellisola G, Sorio C. Infrared spectroscopy and microscopy in cancer research and diagnosis. Am J Cancer Res. 2011 Nov 22;2(1):1–21.

159. McGranahan N, Swanton C. Biological and Therapeutic Impact of Intratumor Heterogeneity in Cancer Evolution. Cancer Cell. 2015 Jan 12;27(1):15–26.

160. Gerlinger M, Rowan AJ, Horswell S, Larkin J, Endesfelder D, Gronroos E, et al. Intratumor Heterogeneity and Branched Evolution Revealed by Multiregion Sequencing. N Engl J Med. 2012 Mar 8;366(10):883–92.

161. Vuletić F, Zajec V, Vuletić LB, Seiwerth S. Intratumoral heterogeneity. Diagn Pathol. 2018 Feb 5;4(1).

11. CURICULLUM VITAE

Fatlinda Sadiku Zehri was born on May 8th, 1980 in Peja, Republic of Kosovo. In 2005 she obtained a Doctor degree in Medicine from the University of Prishtina, Faculty of Medicine, Republic of Kosovo. After six months of obligatory working experience, she passed the state exam. She started a residency program in Cytology at the University of Prishtina, Faculty of Medicine, Department of Anatomic Pathology, and received the title Specialist of Cytology, in October 2013.

Fatlinda is currently employed as a regular teaching assistant at the Department of Histology with Embryology - Faculty of Medicine, University of Prishtina. Also, after completing the continuing education in Cytology, she has been working as a Cytologist, within the Department of Anatomic Pathology at University Clinical Center of Kosovo.

She is mother of two sons.